

copy 2

MAY 21 1970

DEC 2 1970

DEC 02 1986



## RESEARCH ON SURFACE CATALYSIS IN NONEQUILIBRIUM FLOWS

J. A. Bartz and R. J. Vidal

Cornell Aeronautical Laboratory, Inc.

April 1970

TECHNICAL REPORTS  
FILE COPY

This document has been approved for public release and  
sale; its distribution is unlimited.

**ARNOLD ENGINEERING DEVELOPMENT CENTER  
AIR FORCE SYSTEMS COMMAND  
ARNOLD AIR FORCE STATION, TENNESSEE**

PROPERTY OF U. S. AIR FORCE  
AEDC LIBRARY  
F40600-69-C-0001

# ***NOTICES***

When U. S. Government drawings specifications, or other data are used for any purpose other than a definitely related Government procurement operation, the Government thereby incurs no responsibility nor any obligation whatsoever, and the fact that the Government may have formulated, furnished, or in any way supplied the said drawings, specifications, or other data, is not to be regarded by implication or otherwise, or in any manner licensing the holder or any other person or corporation, or conveying any rights or permission to manufacture, use, or sell any patented invention that may in any way be related thereto.

Qualified users may obtain copies of this report from the Defense Documentation Center.

References to named commercial products in this report are not to be considered in any sense as an endorsement of the product by the United States Air Force or the Government.

RESEARCH ON SURFACE CATALYSIS  
IN NONEQUILIBRIUM FLOWS

J. A. Bartz and R. J. Vidal  
Cornell Aeronautical Laboratory, Inc.

This document has been approved for public release and  
sale; its distribution is unlimited.

## FOREWORD

The research reported here was sponsored by the Arnold Engineering and Development Center (AEDC) of the Air Force Systems Command (AFSC) under Contracts No. F40600-68-C-0001 and No. F40600-69-C-0005. This Air Force Program, Element No. 61102F, Project 8951, Task 06, entitled Research and Experimental Study of Surface Catalysis in Nonequilibrium Flows, was performed in the Aerodynamic Research Department of the Cornell Aeronautical Laboratory, Inc. at Buffalo, New York during the period September 1967 to September 1969 under the technical cognizance of Lt. Vincent Rocco, AELR. This report is also identified as CAL Report No. AF-2753-A-2 and was released for publication on 14 November 1969.

This technical report has been reviewed and is approved.

Vincent S. Rocco  
First Lieutenant, USAF  
Research Division  
Directorate of Plans  
and Technology

Harry L. Maynard  
Colonel, USAF  
Director of Plans  
and Technology

## ABSTRACT

This report describes the results of a program of research to develop a catalytic probe with a discontinuous catalytic surface. The ultimate objective is to use the probe to measure the ambient oxygen atom concentrations in high-temperature wind tunnel facilities, and a discontinuous catalytic surface was used to increase the probe sensitivity to small atom concentrations. This report first reviews the theoretical basis for this probe configuration, and then presents experimental data obtained with the probe in air and simulated air. The accuracy of existing theory for a probe with a discontinuous catalytic surface is demonstrated in equilibrium flow experiments in a shock tube using simulated air with a single reactant. Subsequent equilibrium flow experiments in real air indicate that oxygen atom recombination is the only important reaction occurring on the surface and thereby demonstrate the utility of the probe as a diagnostic in high-temperature air flows. Exploratory experiments are described using the catalytic probe in a nonequilibrium flow of air and simulated air produced in a shock tunnel. These results show large discrepancies between theory and experiment, and the possible sources of these discrepancies are discussed. It is concluded that the discrepancies could result from a weak wave system in the nozzle and from uncertainties in the chemical rate data used in the theoretical prediction of the nozzle flow.

## TABLE OF CONTENTS

<u>Section</u>		<u>Page</u>
	FOREWORD . . . . .	ii
	ABSTRACT . . . . .	iii
	LIST OF ILLUSTRATIONS. . . . .	vi
	LIST OF SYMBOLS . . . . .	vii
I	INTRODUCTION . . . . .	1
II	THEORY . . . . .	4
III	APPARATUS AND PROCEDURES . . . . .	7
	Models . . . . .	7
	Shock Tube Experiments . . . . .	8
	Shock Tunnel Experiments . . . . .	9
	Data Reduction . . . . .	11
	Surface Conditioning . . . . .	12
IV	RESULTS FOR EQUILIBRIUM FLOWS . . . . .	13
	Convective Heating . . . . .	14
	Recombination Heating . . . . .	15
	Effect of Catalytic Surface Condition . . . . .	18
V	RESULTS FOR NONEQUILIBRIUM FLOWS. . . . .	20
	Convective Heating . . . . .	21
VI	CONCLUDING REMARKS . . . . .	27
	APPENDIX A - CHEMICAL KINETIC MODEL. . . . .	28
	APPENDIX B - SECOND-ORDER SURFACE REACTIONS . . . . .	30
	REFERENCES . . . . .	33

## LIST OF ILLUSTRATIONS

<u>Figure</u>		<u>Page</u>
1	Theory for Heat Transfer to a Surface with a Discontinuous Catalytic Efficiency - Ref. 7 . . .	36
2a	Small-Scale Catalytic Probe. . . . .	37
2b	Large-Scale Catalytic Probe. . . . .	38
3	Typical Data Obtained with a Catalytic Probe in an Equilibrium Airflow. . . . .	39
4	Variation of the Density-Viscosity Product in Air Across a Boundary Layer (Blasius Profile) . . .	40
5	Convective Heat Transfer to a Flat Plate in Equilibrium Flow . . . . .	41
6	Comparison of Theoretical and Measured Atom Fractions on a Catalytic Surface in Equilibrium Flows . . . . .	42
7	Ambient Oxygen Atom Fractions Inferred with a Catalytic Probe in Equilibrium Flows . . .	43
8	Effect of Preconditioning on the Catalytic Surface .	44
9	Typical Data Obtained with a Catalytic Probe in a Nonequilibrium Airflow . . . . .	45
10	Convective Heat Transfer to a Wedge in Nonequilibrium Flow . . . . .	46
11	Comparison of Theoretical and Measured Atom Fractions on a Catalytic Surface in Nonequilibrium Nozzle Flows - Large-Scale Probe . . . . .	47
12	Comparison of Theoretical and Measured Atom Fractions on a Catalytic Surface in Nonequilibrium Nozzle Flows - Small-Scale Probe . . . . .	48
13a	Survey of Nozzle Flow Uniformity . . . . .	49
13b	Survey of Nozzle Flow Uniformity . . . . .	50
14	The Temporal Variation of Inferred Atom Fraction .	51

## LIST OF SYMBOLS

$A$	parameter governing asymptotic theory, Eq. (2)
$c$	specific heat
$C$	Chapman-Rubesin constant
$C_H$	Stanton number
$D$	diffusion coefficient
$h$	static enthalpy
$h_2$	heat of recombination of atomic oxygen
$H$	total enthalpy, including kinetic and chemically frozen energy
$k$	thermal conductivity
$k_w$	reaction speed on the catalytic surface
$Le$	Lewis number, $\frac{Pr}{Sc}$
$M_s$	incident shock Mach number
$Pr$	Prandtl number
$q$	heat transfer rate per unit area
$q_r$	recombination heat transfer rate per unit area
$Re_x$	Reynolds number, $\frac{\rho_e u_e x}{\mu_e}$
$Sc$	Schmidt number
$t$	time
$T$	temperature
$u$	velocity in the chordwise direction
$U_\infty$	velocity of the ambient stream
$x$	chordwise distance along the surface from the leading edge
$x_0$	chordwise distance from the leading edge to the discontinuity
$y$	distance normal to the surface
$\alpha$	mass fraction
$\gamma$	surface catalytic efficiency
$\mu$	viscosity
$\rho$	density



## LIST OF SYMBOLS (Cont.)

Subscripts

$C$	catalytic surface
$NC$	noncatalytic surface
$e$	condition at the edge of the boundary layer
$w$	condition at the wall
$\infty$	condition in the ambient stream
$O$	atomic oxygen
$NO$	nitric oxide

## I. INTRODUCTION

A program of research has been in progress at CAL to develop a catalytic probe to measure oxygen atom fractions in high-temperature airflows. The basic principle of a catalytic probe is to measure convective heat transfer to a noncatalytic surface and the heat transfer to an adjacent surface known to catalyze atom recombination. The latter will be the sum of the convective heat transfer and the heat released in surface atom recombination. The difference in the heat transferred to the two surfaces is the heat released in atom recombination, which is directly related to the atom fraction in the ambient stream.

The requirement for a catalytic probe stems from the current and planned generation of high-performance test facilities for gas-dynamic testing. Typically, these facilities generate a reservoir of high-temperature, partially dissociated air which is expanded in a nozzle system to a high velocity to duplicate or simulate high-speed reentry conditions. During the rapid expansion, the air cannot remain in thermochemical equilibrium, and the final expanded state is a mixture of atoms and molecules. There are comprehensive machine programs for predicting the final composition of such flows, but their accuracy depends critically on accurate and relevant chemical rate data. The existing rate data is open to considerable question, making it mandatory to obtain a direct measurement of the atom fractions in these facilities. The catalytic probe being developed here is intended to fill an important portion of that need by providing a means for measuring the oxygen atom concentration. Over a wide range of reservoir conditions of interest in such facilities, the energy frozen in oxygen dissociation is a prime contribution to the departure from equilibrium.

In previous research in this program,<sup>1, 2, 3</sup> a catalytic probe was successfully applied to measure atom fractions in simulated air in equilibrium flow experiments and a limited number of nonequilibrium flow experiments.<sup>3</sup> The probe configuration chosen was a flat plate<sup>1</sup> or slender wedge<sup>3</sup> with a catalytic (silver) surface beginning at the leading edge. This slender

configuration suppressed or eliminated complications associated with a blunt-body probe,<sup>4</sup> such as chemical reactions and rarefaction effects in the probe flow field. The data were interpreted within the context of existing theory in the following manner. The experiments were performed under diffusion controlled conditions, which insured that the inferred atom fractions were essentially independent of the surface catalytic efficiency,<sup>1</sup> and therefore a function only of the gasdynamic variables and transport properties. The combination of frozen flow field chemistry and diffusion controlled surface reaction allowed application of conventional thin boundary layer theory.<sup>5,6</sup> The theory,<sup>5,6</sup> when modified to include species distributions,<sup>2</sup> was adequate for complete data interpretation.

With this approach, the applicability of the slender catalytic probe was successfully demonstrated in both equilibrium<sup>1</sup> and nonequilibrium<sup>3</sup> flow experiments. However, the probe sensitivity was marginal when small fractions of energy were frozen in oxygen dissociation in the nonequilibrium expansions.<sup>3</sup> As discussed in the literature, for example Refs. 7 and 8, a method of increasing sensitivity is theoretically possible by locating the leading edge of the catalytic surface behind the leading edge of the body. This displaces the origin of the species boundary layer relative to that for the thermal boundary layer. Consequently, at any point behind the discontinuity in catalytic efficiency, the convective heating is reduced relative to the recombination heating. The probe sensitivity, which is proportional to the difference between the total heating on the catalytic surface and the convective heating on the noncatalytic surface, is therefore increased.

Although the discontinuous catalytic surface theoretically provides the desired sensitivity increase, the inferred atom fraction will in general be a function of the surface catalytic efficiency.<sup>7</sup> This is not a serious limitation, since the catalytic efficiency of silver for oxygen recombination has been measured by a number of investigators.<sup>9,10,11</sup> The value reported by Myerson<sup>11</sup> is used here. In addition, the dependence on catalytic efficiency can be minimized by suitable choice of experimental conditions, as discussed in a succeeding section.

The purpose of the present research is to apply a probe with a discontinuous catalytic surface to the measurement of oxygen atom fractions in equilibrium and nonequilibrium airflows. The intent is to extend the applicability of the catalytic probe to the measurement of small atom fractions, utilizing the potential of sensitivity increase at the discontinuity. The basic experimental method parallels that used in the earlier research<sup>1, 3</sup> in that the probe utility and accuracy is demonstrated first in shock tube experiments where there is a high level of confidence in the fluid dynamic and thermochemical understanding. The shock tunnel experiments were designed to duplicate largely the shock tube conditions, and because of the thermochemical uncertainties in shock tunnel flows, these experiments serve as a check on the knowledge of shock tunnel flows and on the probe performance. The succeeding section summarizes available theory to establish the basis for designing the experiments. This is followed by a discussion of apparatus, procedures, and results.

## II. THEORY

Prior to discussion of the experiments, applicable theory for a discontinuous catalytic surface will be briefly reviewed, to define parameters governing the problem and to establish the basis for the experimental research.

The theory of Simpkins<sup>8</sup> for a discontinuous catalytic surface provides a convenient closed form solution, but is not applicable to the present problem because of the imposed boundary conditions. In that theoretical treatment, the atom fraction at the catalytic wall is set equal to zero, corresponding to the diffusion-controlled limit. Far downstream of the discontinuity, this condition is approached, but near the discontinuity the finite wall reaction speed results in a nonzero atom fraction at the wall. This boundary condition therefore leads to serious error in the vicinity of the discontinuity. In fact, the theory predicts an infinite heat transfer rate at the discontinuity.

The theory of Chung, Liu, and Mirels<sup>7</sup> applies a more appropriate wall boundary condition. A first-order wall reaction of the form

$$\alpha_w = \frac{D_w}{k_w} \left( \frac{\partial \alpha}{\partial y} \right)_w \quad (1)$$

is assumed. This boundary condition results in a wall atom fraction that remains continuous at the discontinuity in catalytic efficiency, and predicts a finite recombination heat transfer rate at the discontinuity. The problem is reduced to a Volterra integral equation which is solved by a series method for a limited range of the governing parameters. In addition, an approximate solution is obtained by a Polhausen integral method for a broader range of the parameters.

The important features predicted by the theory are indicated in Fig. 1, in which the solution obtained with the Polhausen method<sup>7</sup> is shown. The ordinate is the dimensionless recombination heat transfer rate, divided

by the dimensionless energy in dissociation. A value of the ordinate of unity implies that all the energy available in dissociation is recovered on the catalytic surface, corresponding to the case of a continuous catalytic surface in the limit of diffusion-controlled reaction on the surface. The various curves are the theoretical prediction of recombination heating at fixed locations of interest on the catalytic surface. It is clear from the figure that it is theoretically possible to greatly amplify the recombination heat transfer rate with the discontinuity in catalytic efficiency. The ordinate is a direct measure of the amplification in relation to the continuous catalytic surface. This amplification is achieved by reduction of the convective heating, while recovering essentially all of the energy available in dissociation on the catalytic surface. The abscissa is the parameter from the theory for a flat plate that governs the surface reaction. At small values of the parameter, the reaction on the surface is controlled by the reaction speed of the catalyst, while at large values of the parameter, the reaction is controlled by atom diffusion to the surface.

It can be seen that each curve has a local maximum occurring at values of the abscissa of about 15 to 30. This maximum occurs because of a balancing between rate-controlled and diffusion-controlled surface reaction. For small values of the abscissa, the recombination heating will tend to be rate-controlled, and not all of the atoms reaching the surface will recombine, since the surface catalytic efficiency is less than unity. For large values of the abscissa, as the diffusion-controlled limit is approached, atoms will tend to recombine upstream of the location under consideration. Consequently, a maximum in recombination heating occurs. This maximum, which is quite invariant with the abscissa over a fairly wide range, is highly desirable from the experimental standpoint, for the following reason. The abscissa involves the wall reaction speed and the Chapman-Rubensin constant, both of which are subject to some uncertainty, as will be discussed in a later section. An uncertainty in the abscissa in the region of the maximum results in a very small uncertainty in the ordinate. Consequently, recombination heating should be accurately predictable in spite of the uncertainty in the abscissa.

Although this figure illustrates important features of a discontinuous catalytic surface, it can be seen that, in this form, the ordinate is a complicated function of two parameters, the abscissa and  $\chi/\chi_0$ . This complicated dependence is undesirable for the interpretation of experimental results. For this reason, a simplification of theory was developed in the present research. This was done by expanding the leading terms in the series solution of Chung et al.<sup>7</sup> around the discontinuity and retaining a practical number of terms. The result is

$$\frac{\alpha_w}{\alpha_e} = \frac{1 + 2A + \frac{3}{2}A^2 + \frac{3}{5}A^3 + \dots}{(1+A)^4}, \quad A = G \left[ \left( \frac{\chi}{\chi_0} \right)^{3/4} - 1 \right]^{1/3},$$

$$G = \left[ 1.2373 S_c^{2/3} \frac{\rho_w k_w}{\rho_e u_e} \sqrt{\frac{Re_{\chi_0}}{C}} \right]_c \quad (2)$$

The atom fraction at the wall,  $\alpha_w/\alpha_e$ , is related to the ordinate of Fig. 1 through

$$\frac{\frac{q_c - q_{nc}}{q_{nc}}}{L_e^{2/3} \frac{\alpha_e k_p}{H_e - \alpha_e h_p - h_w}} = 2.435 G \frac{\alpha_w}{\alpha_e} \sqrt{\frac{\chi}{\chi_0}} \quad (3)$$

The important feature of the simplification, Eq. (2), is that  $\alpha_w/\alpha_e$  is given as a unique function of a single parameter  $A$ . A comparison of this simplified, asymptotic form of theory showed that it agrees within a few percent with the general solution<sup>7</sup> over the following range:

$$1 \leq \frac{\chi}{\chi_0} \leq 1.5, \quad 1 \leq G \leq 10.$$

The above limits extend well beyond the range of interest of the present experiments. The asymptotic form, Eq. (2), therefore provides the means by which measurements obtained on a discontinuous catalytic surface may be simply and accurately interpreted over a broad range of experimental conditions.

### III. APPARATUS AND PROCEDURES

The present experiments were performed in the CAL Superorbital Shock Tube<sup>1</sup> and the CAL Six-Ft. Hypersonic Shock Tunnel,<sup>3</sup> using air and simulated air as test gases. The simulated air was composed of oxygen diluted with argon, which restricted possible surface reactants to atomic oxygen. In the shock tube experiments, the test gas processed by the incident shock wave equilibrated in a small fraction of the available test time. Consequently, the ambient stream was in thermochemical equilibrium, and its composition could be predicted with a high level of confidence. In contrast, in the shock tunnel experiments, the rapid expansion of the test gas from the reservoir through the nozzle system resulted in appreciable departures from thermochemical equilibrium, and the state of the test gas must be predicted using nonequilibrium machine solutions. The uncertainty in the reaction rate data lends some uncertainty to the gas composition in the model flow field.

#### Models

Two models were employed in the present experiments. The small-scale model, 2 in. wide x 3 in. long, shown in Fig. 2a, was used in both shock tube and shock tunnel experiments. The large-scale model, 6 in. wide x 8.5 in. long, shown in Fig. 2b, was used in the shock tunnel. The only basic difference between the two models is the absolute model scale, as indicated in Fig. 2. Each consists of a steel plate with a pair of Pyrex 7740 glass instrumentation inserts. Each insert contains eight thin-film thermometer gages, nominally 0.35 in. long and 0.010 in. wide. Gage pairs are located equidistant from the leading edge of the model to provide local pairs of values of total and convective heat transfer. The gages are clustered near the discontinuity to provide a detailed survey in the region in which large variations of recombination heat transfer rate are predicted by theory, Fig. 1. The nominal distance from the discontinuity to leading edge of the gages is 0, 0.02, 0.04, 0.08, 0.16, 0.25, 0.40, and 0.60 inches. As indicated in Fig. 2, the location of the discontinuity behind the model



leading edge is 2.0 and 5.4 inches on the small-scale model and the large-scale model, respectively. Model fabrication and instrumentation techniques, including fabrication of the gages, insulation coating on the gages, silver deposition, and heat transfer analog networks are thoroughly discussed in Refs. 1 and 3.

### Shock Tube Experiments

The present shock tube experiments are a direct extension of the experiments reported in Ref. 1, with two important exceptions. First, air was used as a test gas in the present experiments. In Ref. 1, oxygen diluted with various fractions of argon was used to simulate air. This oxygen-argon composition restricted the possible surface reactants to one, atomic oxygen, to eliminate any complication in those initial experiments. Simulated air was also used initially in the present experiments, followed by the experiments in air, as will be discussed in the next section.

The second important difference from Ref. 1 is the use of a discontinuous catalytic surface. Except for this feature, the model size, support, location, etc., were unchanged. The experiments consisted of driving shock waves ( $M_s = 9$  to 15) into the test gas with a heated (750°F) hydrogen driver. The heated test gas established a supersonic flow over the model, which was mounted in an instrumentation collar in the shock tube. The model was pitched at a 5° expansion angle to shield the instrumented surface from particle damage. The various constraints imposed upon the experiment are discussed fully in Ref. 1, so that they will be considered only briefly. To insure an ambient equilibrium composition, the chemical equilibration time behind the incident shock wave must be small in comparison with available test time. This was checked with the machine program developed at CAL for finite-rate chemical relaxation behind a normal shock wave.<sup>12</sup> For the shock tube data reported, the calculated equilibration time never exceeded 20% of the available test time. An additional requirement is that chemical reactions in the model flow field must be frozen. This was checked by hand calculation of the relaxation time in the inviscid layer, and application of reacting boundary layer theory<sup>13</sup>

near the model surface. Other considerations were the dynamic pressure limits imposed by the model support system, the possibility of flow blockage at the model location, the influence of catalytic efficiency, and effects of shock wave attenuation. These various constraints were satisfied in the selection of test conditions for each experiment, in the manner described in Ref. 1. As pointed out in the discussion of Fig. 1, the dependence on surface catalytic efficiency can in general be eliminated by a suitable choice of test conditions. In the present shock tube experiments, however, elimination of this dependence would likely have resulted in a violation of the various constraints. For this reason, the inferred atom fractions that are presented depend weakly on surface catalytic efficiency, as will be subsequently discussed. The effect of shock wave attenuation on the measured heat transfer rates was estimated to be less than 10% in all cases, and was neglected in data reduction.

### Shock Tunnel Experiments

The present shock tunnel experiments employed probes with a discontinuity in catalytic efficiency in nonequilibrium expansions of air and simulated air. The design of these experiments is based largely on previous shock tunnel experiments in simulated air with a continuous catalytic surface.<sup>3</sup> Except for the difference in the test gas and the probe configuration, the basic experiment was unchanged. Consequently, the discussion will emphasize variations from the experiments reported in Ref. 3.

The experiments consisted of driving shock waves ( $M_s = 9$  to 13) into the test gas with a heated (750°F) hydrogen driver. The reservoir condition was produced by shock wave reflection and further compression caused by overtailoring. The test gas in the reservoir was then expanded through a two-stage nozzle system. The nozzle system consists of a two-dimensional throat and contoured supersonic nozzle, which is followed by a 7 1/2° flow-turning wedge to centrifuge particles from the flow. The central core was then expanded through a 10° half-angle conical nozzle, which established a hypersonic flow over the model, suspended in the nozzle.

Two catalytic probes of different scale were used in the present experiments. In the initial experiments, the large-scale probe was positioned in a fixed axial location in the conical nozzle of the shock tunnel. Variations of ambient test conditions were produced by changing the shock tube conditions. Additional experiments were performed with the small-scale model on a sting mount. The model was located at various axial positions in the conical nozzle to provide an additional method of varying ambient conditions. The models were pitched at a compression angle with respect to the nozzle centerline, primarily because the sensitivity near the discontinuity is enhanced at large wedge angles. An angle of  $25^\circ$  was chosen because this angle produces pseudo-equilibrium in the inviscid flow over the model over a rather wide range of ambient conditions. In addition, boundary-layer displacement effects are suppressed by the compression wedge, allowing direct application of the Chung et al solution,<sup>7</sup> which is a thin boundary layer theory. Because of the compressive pitch angle of the small-scale model, it became necessary to add a spanwise and chordwise extension to the model. This extension (2 in. additional span, 1 in. additional chord) eliminated small (10-15%) effects on surface heat transfer rates, which were caused by the finite model chord and span. These effects were not present in the shock tube experiments because the instrumented surface was essentially aligned with the ambient stream.

Pitot pressure was measured in the ambient stream at the axial location of the model leading edge. In association with the probe measurements, transverse stagnation heat transfer surveys were performed at the farthest forward axial station of interest in these experiments. These heat transfer surveys indicated a nonuniformity of about 10% to 15% in the core region of the flow. This result is consistent with other flow surveys in this facility. Transverse pitot pressure surveys,<sup>3</sup> as well as other axial and transverse surveys with pitot probes and stagnation heat transfer gages indicate a nonuniformity of about  $\pm 10\%$  for this primary-secondary nozzle combination.

## Data Reduction

For the shock tube experiments, the ambient stream conditions were computed from the initial test gas conditions and the incident shock wave velocity, obtained from transit time data. A CAL machine program for normal shock waves was used to compute the equilibrium species composition and gasdynamic properties from the initial conditions. Properties at the edge of the model boundary layer were calculated by applying a small ideal gas correction to the ambient conditions to account for the 5° expansion angle of the surface. The method of evaluating transport properties for a mixture of species at various temperatures is discussed in Ref. 1. Deexcitation of the vibrational energy mode through the model boundary layer was not accounted for in the data reduction.

For the shock tunnel experiments, the ambient stream conditions were calculated from a machine program developed at CAL for finite-rate nozzle expansions of reacting gases.<sup>14</sup> The chemical kinetic model chosen for this calculation is described in Appendix A. Briefly, the model includes ten reaction mechanisms among six neutral air species, with reaction rates based upon high-temperature experiments in dissociating gases. Reservoir conditions were computed using standard data reduction techniques<sup>3</sup> and supplied as input data for the machine program. For the finite-rate calculation, it was assumed that vibrational energy remained in equilibrium in the primary nozzle expansion, and froze at the Prandtl-Meyer fan which turns the flow. Calculations employing finite-difference vibrational relaxation methods<sup>15</sup> confirmed that this assumption regarding vibrational freezing is reasonable. Further, these calculations indicated that the uncertainty in the frozen vibrational energy is energetically unimportant for the present experiment. The ambient stream conditions were calculated from the finite-rate machine solution which was continued to the measured pitot pressure. Properties at the edge of the model boundary layer were calculated from ideal gas oblique shock wave relations. Excitation of the vibrational energy mode in the model flow field was estimated to be energetically negligible over the instrumented model length. Heat transfer data obtained with catalytic probes in the shock tunnel were

corrected for a source flow effect, created by the source-like expansion in the conical secondary nozzle. The method of applying the correction is described in Ref. 3. The corrections amounted to a maximum of 14% on the absolute heat transfer rates. The inferred atom fraction depends weakly on the source flow effect. This dependence arises because the recombination heating is governed by a parameter that is different from that governing the convective heating. The effect amounted to a maximum of 9% on the parameter,  $G$ , and was neglected.

### Surface Conditioning

The procedure of conditioning a silver surface with a flux of atomic oxygen to produce a catalytic surface has been thoroughly described in Refs. 1 and 3 for shock tube and shock tunnel experiments. Because of the increased importance of surface condition in the present experiments, the condition of the catalytic surface was frequently checked immediately prior to the experiment. This was accomplished by conditioning the surface and then performing the remaining pre-experimental procedure without removing the conditioning apparatus from the system. At the time corresponding to shock tube diaphragm rupture, the conditioning apparatus was pulsed instead, to determine if the silver surface was still catalytic.

In the present shock tube experiments, no alteration of previous techniques<sup>1</sup> was necessary, and no loss in catalytic efficiency after conditioning was observed. In initial experiments in the shock tunnel, however, an invisible layer of oil was deposited on the model by a faulty diffusion pump, causing loss of catalytic recombination on the silver surface. After this condition was corrected, no further indication of contamination was observed.

#### IV. RESULTS FOR EQUILIBRIUM FLOWS

The intent of the shock tube experiments in the present research was to obtain a clear and uncompromised demonstration of the probe's accuracy and utility. For this reason, all complicating factors were avoided in the design of the experiment. The test gas chosen for the initial experiments was simulated air, oxygen diluted with 0.5 mole fraction argon. These choices limited the experiment to a known ambient composition with a single possible surface reactant. The comparison of these experiments with theory was found to be entirely satisfactory, and the emphasis was immediately focused and remained on experiments in air. The airflow experiments were designed to vary ambient conditions over a broad range, without violating any constraints imposed on the experiment, as previously discussed. In the air experiments reported here, the ambient stream was equilibrated in less than 20% of the available test time, and chemical reactions in the model flow field were essentially frozen over the entire model length.

A typical set of unreduced data obtained in an equilibrium air experiment is shown in Fig. 3. These data clearly demonstrate the large increase in sensitivity produced by the discontinuity. The difference between heat transfer rates that corresponds to the diffusion controlled limit is indicated on the right side of the figure. This difference represents the maximum difference attainable at this test condition with a continuous catalytic surface. Near the discontinuity, the difference is about ten times the value corresponding to the continuous catalytic surface, demonstrating the practical amplification obtainable with a catalytic discontinuity.

Analysis of the shock tube data obtained with catalytic probes will center on testing applicable theory<sup>7</sup> for a discontinuous catalytic surface. The appropriate starting point is the analysis of the convective heat transfer data obtained on the noncatalytic surface.

## Convective Heating

Although the Chung et al theory<sup>7</sup> is applicable to the present experiments, it relies upon an assumption that is inaccurate for the present case. The theory accounts for variations in the density-viscosity product through the boundary layer by assuming viscosity varies linearly with temperature. The viscosity is then matched to the ambient and wall conditions, resulting in the introduction of the Chapman-Rubesin constant as a parameter. Although this approximation is routinely applied, it is shown in Ref. 1 that the approximation can produce serious errors in high-temperature flows.

The inaccuracy of the Chapman-Rubesin approximation at high temperatures is illustrated in Fig. 4, for a set of conditions approximately corresponding to the present experiments. The variation of the density-viscosity product across an equilibrium (Blasius) boundary layer is shown for three different temperature conditions. The result labelled exact is obtained by locally computing the density and viscosity at the corresponding temperature. The Chapman-Rubesin approximation can be seen to be valid only at the wall condition, and in serious error throughout the remainder of the boundary layer. The approximate method of Refs. 1 and 2, obtained by matching the density-viscosity product at two points in the boundary layer, can be seen to be in good agreement with the result labelled exact through the entire boundary layer. In Ref. 2, Crocco theory<sup>5,6</sup> is modified to include the variation of the density-viscosity product. It is shown in Ref. 1 that the modified Crocco theory is in agreement with experiment within about  $\pm 10\%$ , while theory based on the Chapman-Rubesin approximation typically departs by 40%.

A comparison of the present experimental results is made with the Chung et al theory and the modified Crocco theory in Fig. 5. The data include measurements in air, simulated air composed of oxygen diluted with 0.5 mole fraction argon, and limited data in nitrogen diluted with 0.5 mole fraction argon, over a wide range of ambient conditions. It can be seen that the modified Crocco theory, evaluated for representative test conditions, agrees with experiment within about 10%. The Chung et al

theory, also evaluated for representative test conditions,  $C_{nc} = 2$ , overestimates heat transfer by about 40%. Of perhaps most interest here, the Chung et al theory, evaluated for  $C_{nc} = 1$ , provides a good prediction of convective heat transfer rate over a wide range of conditions. The empirical result,  $C_{nc} = 1$ , provides a reasonable basis for applying the Chung et al theory in the interpretation of recombination heating data. The evaluation of  $C_c$  cannot be made readily using the same technique, since the density-viscosity product depends on the wall atom fraction, which is unknown a priori. The method adopted consists of choosing

$$(C_c)_{\text{effective}} = \frac{C_c}{C_{nc}}, \text{ where } C_c \text{ and } C_{nc} \text{ are}$$

evaluated at the experimental conditions. This method tends to preserve the accuracy obtained empirically with the noncatalytic data, and yet allows for the nonzero wall atom fraction on the catalytic surface. Although the method is not rigorous, it provides a reasonable basis for applying the Chung et al theory to analyze data obtained on the catalytic surface.

### Recombination Heating

A critical test of the Chung et al theory can be made by directly comparing the theoretical prediction of wall atom fraction with experiment. The wall atom fraction can be inferred from the measured heat transfer rates by the use of

$$\alpha_w = \frac{q_d}{\rho_w k_w h_D} \quad (4)$$

Estimates with modified Crocco theory indicate that the recombination heat transfer rate on the catalytic surface,  $q_d$ , can be approximated within about 1% accuracy for the present experiments by

$$q_d \approx q_c - q_{nc} \quad (5)$$



This approximation expresses the fact that the difference in convective heating between the catalytic and noncatalytic surfaces, which is dependent on differences in transport properties, is small and may be neglected in inferring atom fractions in the present experiments.

A comparison of theory and experiment is shown in Fig. 6. The asymptotic form of the Chung et al theory, Eq. (2), is plotted versus the governing parameter defined with Eq. (2). The governing parameter was evaluated with  $\gamma_c = 0.12$ , as recommended by Myerson,<sup>11</sup> and the Chapman-Rubesin constant was evaluated following the procedure described earlier. The ordinate is the wall atom fraction normalized by the calculated ambient fraction. Experimental values of the ordinate were computed from Eqs. (4) and (5). Both the ordinate and abscissa were initially evaluated for a perfectly catalytic wall. An iteration was then performed, using the inferred value of  $\alpha_w$ , to correct the initial values and reflect a non-zero wall atom fraction on the catalytic surface. The iteration converged very rapidly, and in no case altered either ordinate or abscissa by more than 10%.

The agreement between theory and experiment in Fig. 6 demonstrates several important points. First, in the experiments with the argon-oxygen gas mixtures, there is only one possible reactant and hence the catalytic wall reaction should be first-order, as assumed in the theory. The good agreement between theory and these data demonstrate the basic accuracy of the theory and confirms the suitability of the values used for the catalytic efficiency and the Chapman-Rubesin constant.

The table in Fig. 6 indicates that in the air experiments, there were two potential reactants present, atomic oxygen and nitric oxide. There is no information in the literature on catalytic wall reactions for a gas mixture of O and NO, but the known gas-phase reactions suggest a plausible wall reaction mechanism. This mechanism and the resulting effect on the present experiments are discussed in Appendix B. If the nitric oxide were affecting the wall reaction, the net result would be to change the order of the wall reaction from a first-order reaction to either a second-order

reaction involving O and NO or a second-order reaction involving just O. That would be the ideal effect. More realistically, the wall reaction would probably be of an order intermediate between one and two, and involving O and NO. In either event, the parameter governing the wall reaction would change from that shown in Fig. 6 and would be proportional to the mass of the reactants entering into the wall reaction,  $\rho_w \alpha_o$  and

$\rho_w \alpha_{no}$ . Consequently, a consistent correlation would not be obtained between the air experiments within the parameter used in Fig. 6. The fact that a consistent correlation is obtained in Fig. 6 for the air data leads to the conclusion that the nitric oxide was not reacting on the surface and that the only important reaction on the surface was oxygen recombination.

The last observation to be made in connection with Fig. 6 is that in the air experiments there was a 1% to 2% mass fraction of NO. This is comparable with the NO mass fraction in nozzle expansions. The shock tunnel experiments, to be discussed in a subsequent section, had NO mass fractions of 2% to 6%. Hence, the ambient condition in these shock tube experiments are comparable with the ambient conditions found in nozzle expansions of air.

To illustrate the potential of a probe with a discontinuous catalytic surface as a diagnostic device, ambient atom fractions were inferred from the data shown in Fig. 6. These are compared to the corresponding computed equilibrium fractions in Fig. 7. The inferred fractions were obtained by a best fit of the experiments to theory, with equal weighting given to each gage. The agreement of the measured values with the accurately calculated equilibrium values is generally within 5%. The greatest departures occur for the experiments at high incident shock Mach numbers. Shock wave attenuation and ionization effects at these conditions could be the source of the small discrepancies indicated. The agreement indicated by Fig. 7 clearly shows the potential of the discontinuous catalytic surface for diagnostic applications.

### Effect of Catalytic Surface Condition

As discussed previously, a potential disadvantage of a discontinuous catalytic surface is that the inferred atom fractions are in general a function of the catalytic efficiency of the surface. With this functional dependence, the inferred atom fractions could therefore be influenced by the history of the catalytic surface. Drift tube experiments<sup>11</sup> indicate that the catalytic efficiency of silver for atomic oxygen recombination is invariant with exposure to atomic oxygen, after an initial exposure of about  $3.5 \times 10^{17}$  atoms/cm<sup>2</sup>. Consequently, in data reduction, the catalytic efficiency can be regarded as a fixed, known value. To provide an even more reliable framework in which to interpret data, however, the invariance of the inferred atom fraction with surface condition was demonstrated in shock tube experiments under the high enthalpy, high velocity conditions of interest.

These shock tube experiments were performed with oxygen diluted with argon as the test gas. The shock tube conditions were unchanged for each of the experiments, but the catalytic surface condition was varied over a wide range. In the first experiment, the silver had no contact with atomic oxygen prior to the flux of the dissociated oxygen in the test gas during the experiment. Following the first experiment, newly deposited silver was exposed to about  $4 \times 10^{17}$  atoms/cm<sup>2</sup>, produced by one pulse of the conditioning apparatus. This exposure was sufficient to discolor the bright silver surface to a faint yellow. The second experiment was then performed. Following the second experiment, the silver surface was exposed to about  $10^{19}$  atoms/cm<sup>2</sup>, produced by a series of pulses from the conditioning apparatus. This exposure was sufficient to severely discolor and dull the silver. The third experiment was then performed. The measured recombination heat transfer rates in these experiments, reduced to the form of inferred atom fractions, is compared to theory in Fig. 8. The second experimental condition was subsequently repeated, and the repeat experiment is included for comparison. It can be seen that within data scatter, the inferred atom fraction is invariant with surface condition, over an extreme range of surface condition. For the first experiment, with no prior exposure of the silver to atomic oxygen, the atom flux during

the test time was sufficient to condition the silver. Consequently, the first experiment agrees with the second and third. Although invariance may be expected from the drift tube results, these shock tube data obtained under high enthalpy conditions add confidence to the data interpretation. In Fig. 8, both ordinate and abscissa of the experimental data points were computed using Myerson's<sup>11</sup> value of  $\gamma_c = 0.12$ . The agreement between theory and experiment indicated in Fig. 8 support this value, but because of the empiricism involved in the determination of  $C_c$ , no attempt was made to infer a catalytic efficiency from any of the present data.

In summary, the shock tube experiments with air and with simulated air show that a probe with a catalytic discontinuity provides an amplified sensitivity to oxygen atom concentrations which is as much as ten times greater than that with a continuous catalytic surface. The data obtained in simulated air, having a single reactant, provides a valid test of the theory for the probe and demonstrates that the theory can be accurately applied to infer the ambient atom concentrations. In the experiments with real air, there were two potential reactants present, atomic oxygen and nitric oxide. The data agree well with the theory for a first-order wall reaction, thereby indicating that the nitric oxide did not influence the wall reaction.

## V. RESULTS FOR NONEQUILIBRIUM FLOWS

The equilibrium experiments in the shock tube provided the necessary verification of theory<sup>7</sup> for a discontinuous catalytic surface, and demonstrated that the probe can be used to measure oxygen atom concentrations in dissociated air. With this completed, attention next was focused on applications with this probe configuration in nonequilibrium shock tunnel experiments. In the design of the initial nonequilibrium experiments, emphasis was placed on maximizing the increase in probe sensitivity produced by the discontinuity. For this reason, a probe of larger scale, pitched at a compression angle, was chosen for the experiment, since this configuration theoretically produces a large sensitivity to ambient atom fraction. The results of these experiments did not agree with theory, and it was thought initially that the discrepancies were caused by gas-phase recombination in the boundary layer of the probe. Consequently, a second series of shock tunnel experiments was performed, with the emphasis placed on largely duplicating conditions of the equilibrium shock tube experiments. The small-scale model used in the equilibrium experiments was employed, and conditions at the edge of the model boundary layer were duplicated approximately by adjusting both reservoir conditions and the model location in the nozzle.

A typical set of data recorded in a nonequilibrium expansion of air is shown in Fig. 9. These data were obtained with the small-scale model, modified with an extension as previously discussed. The general trends exhibited by these data are similar to the trends in the equilibrium experiments, Fig. 3. As in the equilibrium case, these data again clearly demonstrate the large sensitivity increase produced by the discontinuity. Referring to the diffusion-controlled limit on the right side of the figure, it can be seen that the sensitivity at the discontinuity is increased by a factor of about five. The sensitivity increase is of particular advantage at this test condition, since the computed value of ambient atom mass fraction is only 0.068.

## Convective Heating

In the discussion of the equilibrium data, it was demonstrated that the convective heat transfer data were in good agreement with theory,<sup>2</sup> and that the theory for convective heat transfer given by Chung et al.<sup>7</sup> agreed well with the data if the Chapman-Rubesin constant was taken to be unity. In the nonequilibrium flow experiments, however, it was found that the convective heat transfer data is generally not in agreement with theory. This is illustrated in Fig. 10, where representative data from the nonequilibrium experiments are compared with applicable theory. The data shown were obtained with the large-scale model and small-scale model (with the extension) at reservoir temperatures ranging from 5400 to 6100°K. The test gases were air and simulated air. It can be seen that except for three experiments, the data fall about 50% above the theory. It should be emphasized that conditions in the model flow field were not drastically different from those in the equilibrium shock tube experiments. Consequently, it is difficult to attribute the discrepancies to any theoretical approximation, such as the Chapman-Rubesin constant.

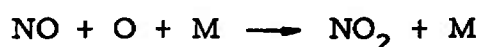
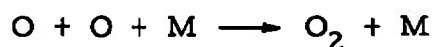
The data obtained with the large-scale and the small-scale models have been used to infer the ambient atom fractions. These are compared with theory<sup>7</sup> in Figs. 11 and 12. The data obtained with the large-scale model fall generally below theory with no distinct trends apparent. Only two experiments with the small-scale model are reported here, Fig. 12. The others were influenced by finite-span and finite-chord effects of 10% to 15%, which only confuse the issue. It can be seen that the data from these two experiments are in reasonable agreement with theory, even though the data for the convective heat transfer, Fig. 10, are substantially above the theory.

The source of the observed discrepancies is not apparent, though there are a number of possibilities. These include 1) boundary layer displacement effects, 2) gas-phase recombination in the boundary layer, 3) higher-order wall reactions, 4) effects associated with a discontinuous surface temperature, 5) disturbances in the ambient stream, 6) erroneous

rate data for predicting the ambient atom concentration, and 7) contaminants in the test gas. These will be discussed in that order.

Boundary Layer Displacement Effects. The trends evident in Fig. 10 qualitatively are consistent with boundary layer displacement effects. Cheng's theory<sup>16</sup> for the combined effects of wedge angle and boundary layer displacement was used to check this possibility. Although the ambient viscous interaction parameter was large,  $\bar{\chi} \approx 80$ , the wedge effects dominated the heat transfer and the calculated displacement effects never exceed 2%.

Gas-Phase Recombination. The trends in Figs. 10, 11, and 12 are also consistent with the effects of gas-phase recombination in the boundary layer in that this mechanism would consume oxygen atoms and increase the convective heat transfer to the surface. There are no known solutions that apply directly to this problem. Consequently, an existing theory for dissociation in the boundary layer of a flat plate<sup>17</sup> was extended to account for recombination. This theory, reported in Ref. 13, was applied here to estimate recombination effects. It was found that both three-body oxygen atom recombination and nitric oxide three-body recombination would be important.



The role of these reactions was examined for the present experiments using the rate data given in Ref. 18 and it was concluded that gas-phase recombination would alter the inferred atom fraction by about 3%.

Higher-Order Wall Reactions. A partial basis is outlined in Appendix B for considering wall reactions that are other than first-order. It is possible to extend existing theory<sup>7</sup> to allow for higher-order reactions, but the application of the theory would depend upon obtaining rate data for the reactions. This difficulty was circumvented by generalizing the parameter that governs the wall reaction, defined in Eq. (2), to allow for a second-order wall reaction.

$$G_2 = 1.2373 S_c^{2/3} \frac{\rho_w^2 \alpha_1 \alpha_2}{\rho_e u_e \alpha_1} \sqrt{\frac{R_{ex}}{C}}$$

In the above relation,  $\alpha_1$  and  $\alpha_2$  are mass fractions of the two reacting species, and it is assumed  $\alpha_1$  is the only reactant adsorbed on the surface. The possibility of second-order reactions influencing the results can be tested by scaling the data in Figs. 11 and 12 with respect to one experiment. A consistent correlation within the above parameter would indicate a second-order wall reaction. This scaling was attempted assuming  $\alpha_1$  corresponded to the atomic oxygen and assuming  $\alpha_2$  corresponded first to atomic oxygen and then nitric oxide. It was found that the data from the large-scale model, Fig. 11, could be correlated with good accuracy assuming a second-order reaction in atomic oxygen, but the data from the small-scale model would not fit the correlation. This lack of correlation might be attributed to differences in scale. Consequently, the data obtained with the small-scale model, Fig. 12, were correlated with the shock tube data, Fig. 6, using the above parameter. It was found that a consistent correlation could not be obtained. It should also be noted that this mechanism would leave the discrepancies in convective heat transfer unexplained. From this evidence, it is concluded that the wall reaction in the shock tunnel experiments was not second order.

Discontinuous Surface Temperature. The models used in this research, Fig. 2, had the instrumentation deposited on a glass insert and mounted in the steel flat plate. This chordwise change in materials leads to chordwise discontinuity in surface temperature during the experiments. Under steady conditions, the surface temperature on the model is

$$T \approx 2q \sqrt{\frac{t}{\pi k \rho C}}$$

and the temperature ratio between the glass (G) and the metal (M)

$$\frac{T_g}{T_m} = \sqrt{\frac{(k \rho C)_m}{(k \rho C)_g}}$$



which for Pyrex glass and steel, amounts to a factor of about 8.

The effects of this discontinuous surface temperature on indicated heat transfer was calculated using the Chapman and Rubesin solution<sup>19</sup> given by Eckert and Drake.<sup>20</sup> It was found that the effects would be confined to the immediate vicinity of the discontinuity, and would never exceed 2% to 3% in the present experiments.

Ambient Stream Disturbances. Early research in the CAL 6-ft. shock tunnel disclosed a wave system in the nozzle that influenced the heat transfer measured on test models. The strength of this wave system was decreased to an acceptable level by lowering the Mach number at the entrance to the conical nozzle, but no attempt has been made to completely eliminate the waves. The flow uniformity was checked in earlier research<sup>3</sup> and again during the present experiments using a rake of probes instrumented with stagnation heat transfer gages. It was found that the stagnation heat transfer varied by about 10% to 15% across the nozzle. Typical surveys are shown in Fig. 13. For reference purposes, the location of the model leading edge and the pitot pressure transducer are indicated. It can be seen that at the location of the pitot pressure transducer, in one instance the stagnation point heat transfer is about 9% lower than on the nozzle centerline, and in the other it is about 14% higher.

In order to interpret these data, it was assumed that the difference between the stagnation point heat transfer measured on the nozzle centerline and that at the location of the pitot transducer were caused by a weak oblique compression wave. The stagnation point heat transfer measurements were then used to calculate the strength of the wave, and that result was then used to estimate the effect the wave would have on convective heat transfer to a wedge. It was found that the -9% difference in Fig. 13a would correspond to a -16% change in wedge heat transfer and a +6 1/2% change in  $\sqrt{Re_x}$ . The +14% difference in Fig. 13b would correspond to a +29% change in wedge heat transfer and a -6% change in  $\sqrt{Re_x}$ . These calibrations were made in conjunction with the small-scale model experiments, and can be applied only to those data. The effect in Fig. 10 would

be to bring the data from those two experiments to within 15% to 25% of theory. A similar calculation for the effects of a weak compression wave on recombination heat transfer shows that a -9% and +14% effect on stagnation point heat transfer corresponds respectively to a -22% and +44% effect on inferred atom fraction and a +15% and -20% effect on the governing parameter. This correction tends to bring the data for these two experiments into better agreement with theory.

It should be emphasized that the above discussion assumes the surveys in Fig. 13 are accurate and repeatable. Typically, the scatter in heat transfer is  $\pm 10\%$ , which is comparable to the uncertainty in Fig. 13. The only firm conclusion that can be made is that wedge heat transfer and recombination heat transfer are 2 to 3 times more sensitive to weak waves than stagnation point heat transfer. The small nonuniformities in the flow indicated by the surveys could account for some of the larger discrepancies in the catalytic probe data.

Reaction Rate Data. Another factor that could lead to the discrepancies between theory and experiment in Figs. 10, 11, and 12 is the theoretical prediction of the ambient stream composition. This would affect the convective heat transfer through the energy frozen in dissociation and affect directly the comparison with the inferred atom fraction. The theoretical prediction of the oxygen atom concentration is always open to question because of the uncertainties in reaction rate data. In fact, it was this uncertainty that led to the present effort to develop a catalytic probe. The reaction rate data used is discussed in Appendix A, and it is regarded as probably the best presently available. However, it is recognized that it can be in error and some of the discrepancies in Figs. 10, 11, and 12 must stem from erroneous rate data. However, all of the scatter cannot be attributed to this effect because there is not enough energy in dissociation and vibration to produce the 50% discrepancies observed in the convective heat transfer, Fig. 10.

Test Gas Contamination. The discrepancies between theory and experiment could be a result of test gas contamination by the driver gas.

These experiments were made with shock tube conditions that were far from the ideal tailored interface conditions, and contamination is possible. It should be noted, however, that these test conditions had been used successfully in previous experiments<sup>21</sup> with no indication of gaseous contamination. If contamination were to occur, it would be characterized by combustion in a diffuse interfacial region which would increase the total enthalpy of the gas and deplete the oxygen atom concentration. The oxygen concentration would then decrease as a function of time during the test.

A check on possible contamination was made by forming the ratio,  $\frac{q_c - q_{nc}}{q_{nc}}$ , from a typical experiment and plotting it as a function of time. This ratio of heat transfer rates is proportional to the ambient atom concentration and should reflect the results of any contamination. The oscillograph record and this ratio of heat transfer rates are shown in Fig. 14. It can be seen that for the first 0.8 to 0.9 milliseconds, the ratio of heat transfer rates scatters about the abscissa, reflecting the scatter in the oscillograph record and indicating essentially no oxygen atoms. The indicated atom fraction increases rapidly after 0.9 milliseconds and indicates a fairly constant value for about 1/4 millisecond, and then indicates a sudden decline at the end of the experiment. If anything, the atom fraction increases with time and this behavior is not consistent with driver gas contamination. On this basis, it is concluded that the experiments were not affected by driver gas contamination.

To summarize the above discussion, the shock tunnel experiments disclosed large discrepancies between theory and experiment for convective heat transfer to the probe and for oxygen atom fractions inferred from the probe measurements. Seven potential sources of these discrepancies were examined and all but two were eliminated. It appears that these discrepancies could stem from a system of weak waves in the nozzle of the 6-ft. shock tunnel and from uncertainties in theoretical predictions for the ambient oxygen atom concentrations.

## VI. CONCLUDING REMARKS

The research reported here was directed toward developing a slender probe with a discontinuous catalytic surface to determine the oxygen atom fractions in nozzle expansions of high-temperature air. A discontinuous catalytic surface was used, in preference to a continuous catalytic surface, to increase the probe sensitivity to small oxygen concentrations.

The initial experiments with the probe were made in a shock tube using simulated air and real air. The shock tube was chosen because the test conditions can be selected to insure that the flow is in thermochemical equilibrium. In the first experiments, the test gas was a mixture of argon and oxygen and hence there was only one reactant. These experiments demonstrated the accuracy of theory<sup>7</sup> and thereby provided a sound basis for experiments in air. In the air experiments, there were two possible reactants, atomic oxygen and nitric oxide. These data agree well with theory<sup>7</sup> and with the data obtained in argon-oxygen mixtures. This agreement indicates that the only reactant entering into the wall reaction is oxygen, and that the wall reaction in dissociated air remains a first-order reaction. These shock tube results, by themselves, demonstrate the utility and accuracy of the catalytic probe for high-temperature air flows. The ambient compositions in the shock tube experiments with air are characteristic of those in high-temperature nozzle expansions of air, containing 1% - 2% nitric oxide mass fractions as compared with 2% to 6% in nozzle flows. The lack of a nitric oxide wall reaction in the shock tube experiments indicates there should be none in a nozzle experiment.

A series of experiments was performed with two probes in the nozzle of the CAL 6-ft. shock tunnel using air and simulated air. The convective heat transfer in these experiments was about 50% greater than theory and the inferred atom fraction scattered below theory. The subsequent data analysis suggests that these discrepancies could stem from a system of weak waves known to be in the nozzle and from uncertainties in reaction rate data, but no firm conclusions can be reached with the available data.

## APPENDIX A

### CHEMICAL KINETIC MODEL

The chemical kinetic model chosen for the nozzle nonequilibrium calculations is identical to that of Ref. 14. The reaction mechanisms and rate constants for this model are summarized in Table I. The mechanisms considered are three-body recombination reactions, the nitric oxide "shuffle reactions", and the direct formation of nitric oxide from molecular nitrogen and oxygen. These include all of the important reactions that occur among the six neutral species of the air model.<sup>14</sup> Since the degree of ionization is relatively small, and since the ionization kinetics have little influence on the flow thermodynamics,<sup>14, 16</sup> only neutral species are included in the model.

The rate constants of Ref. 14 are taken directly from Ref. 22. The rates are derived from the summary of experimental data given in Ref. 22. The values for three-body recombination are based upon experiments by Byron<sup>23</sup> and by Wray et al.<sup>24</sup> Values for the shuffle reactions are based on experiments by Wray et al.<sup>24</sup> and Glick et al.,<sup>25</sup> and the rate for direct nitric oxide formation was calculated by Wray<sup>26</sup> from experimental data. In Ref. 22, a comparison of these rate constants with composite values proposed by Wray<sup>26</sup> indicated generally good agreement for the important reactions. It was pointed out, however, that considerable uncertainties exist in the experimental rate data in some cases.<sup>22</sup>

TABLE I  
CHEMICAL KINETIC MODEL

i	Reaction	M	$A_i$	$\eta_i$	$E_i(\text{cal/mole})$
1.	$\text{N}_2 + \text{M} \rightleftharpoons 2\text{N} + \text{M}$	$\text{N}_2$	$3.0 \times 10^{21}$	-1.5	$2.2499 \times 10^5$
2.	$\text{N}_2 + \text{M} \rightleftharpoons 2\text{N} + \text{M}$	N	$1.5 \times 10^{22}$	-1.5	$2.2499 \times 10^5$
3.	$\text{N}_2 + \text{M} \rightleftharpoons 2\text{N} + \text{M}$	$\text{O}_2, \text{O}, \text{NO}, \text{Ar}$	$9.9 \times 10^{20}$	-1.5	$2.2499 \times 10^5$
4.	$\text{O}_2 + \text{M} \rightleftharpoons 2\text{O} + \text{M}$	$\text{O}_2$	$3.6 \times 10^{21}$	-1.5	$1.1796 \times 10^5$
5.	$\text{O}_2 + \text{M} \rightleftharpoons 2\text{O} + \text{M}$	O	$2.1 \times 10^{18}$	-0.5	$1.1796 \times 10^5$
6.	$\text{O}_2 + \text{M} \rightleftharpoons 2\text{O} + \text{M}$	$\text{N}_2, \text{N}, \text{NO}, \text{Ar}$	$1.2 \times 10^{21}$	-1.5	$1.1796 \times 10^5$
7.	$\text{NO} + \text{M} \rightleftharpoons \text{N} + \text{O} + \text{M}$	all species	$5.2 \times 10^{21}$	-1.5	$1.4996 \times 10^5$
8.	$\text{O}_2 + \text{N} \rightleftharpoons \text{NO} + \text{O}$		$1.0 \times 10^{12}$	0.5	$6.200 \times 10^3$
9.	$\text{N}_2 + \text{O} \rightleftharpoons \text{NO} + \text{N}$		$5.0 \times 10^{13}$	0.0	$7.552 \times 10^4$
10.	$\text{N}_2 + \text{O}_2 \rightleftharpoons 2\text{NO}$		$9.1 \times 10^{24}$	-2.5	$1.2912 \times 10^5$

$$k_{f_i} = A_i T^{\eta_i} \exp(-E_i/R_o T)$$

$$\left[ k_{f_i} \right] = \frac{\text{cm}^6}{\text{mole}^2 \cdot \text{sec}} \quad (i = 1-7)$$

$$\left[ k_{f_i} \right] = \frac{\text{cm}^3}{\text{mole} \cdot \text{sec}} \quad (i = 8-10)$$

## APPENDIX B

### SECOND-ORDER SURFACE REACTIONS

The theory of Chung, Liu, and Mirels<sup>7</sup> for a flat plate with a discontinuous catalytic surface implicitly assumes the ambient gas contains a single reactant. In this case, the appropriate derivation for the wall boundary condition<sup>27</sup> can be obtained by assuming equilibrium adsorption on the surface. The relation for the fraction of the surface which is covered by the adsorbed gas,  $\theta$ , is

$$\theta = \frac{K_i p_i}{1 + K_i p_i} \quad (\text{B-1})$$

where  $K$  is the ratio of rate of adsorption to the rate of desorption, and  $p_i$  is the partial pressure of the species  $i$ . The rate of species consumption at the wall is proportional to the fraction of the surface area covered and is expressed as

$$\dot{j}_{w,i} = k_i \theta = \frac{k_i K_i \rho \alpha}{1 + K_i \rho \alpha} \quad (\text{B-2})$$

where  $K_i = K_1 \frac{RT}{M_i}$  and  $M_i$  is the molecular weight of the reacting species. The usual approach is to assume  $K_i \rho \alpha \ll 1$  which is equivalent to assuming  $\theta \ll 1$ ; that is, a sparsely covered surface. The product,  $k_i K_i$ , is also lumped into a single wall reaction rate constant,  $k_{w,i}$ , and the mass rate of species consumption at the wall is equated to mass flux of atoms to the wall in order to obtain the familiar first-order boundary condition,

$$\rho_w D_w \frac{\partial \alpha}{\partial y} = k_{w,i} \rho_w \alpha_w \quad (\text{B-3})$$

When the wall boundary condition is applied in the theory of Ref. 7, it leads to the following similarity parameter governing the wall reaction

$$G_1 = 1.2373 S_c^{2/3} \frac{\rho_w k_w}{\rho_e u_e} \sqrt{\frac{R_{ex}}{C}} \quad (B-4)$$

The derivation when there are two reactants present parallels that for a single reactant and can be found in Ref. 27. Specializing that derivation to a sparsely covered surface, it can be shown that the fraction of the surface covered by the adsorbed species,  $\alpha_1$ , is  $\theta_1 \approx K_1 p_1 = K_2 \rho \alpha_1$ . If the wall reaction is between an adsorbed species,  $\alpha_1$ , and a different gaseous species,  $\alpha_2$ , the mass rate of consumption would be proportional to  $\theta_1$  and the partial pressure of the second reactant.

$$\dot{f}_{w_2} = k_2 p_2 \theta_1 = k_{w_2} \rho^2 \alpha_1 \alpha_2 \quad (B-5)$$

The appropriate boundary condition corresponding to a second-order wall reaction is obtained by equating the above mass rate of consumption to the mass flux of atoms to the wall.

$$\rho_w D_w \frac{\partial \alpha_i}{\partial y} = k_{w_2} \rho^2 \alpha_1 \alpha_2 \quad (B-6)$$

It should be noted that the same equations are obtained if the wall reaction takes place between two adsorbed particles, the Langmuir-Hinshelwood mechanism, because the derivation is restricted to sparsely coated surfaces.

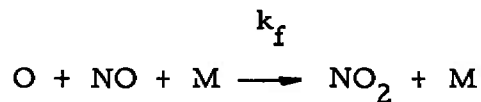
The role of second-order wall reactions in the present experiments can be tested using similarity variables. The appropriate similarity variable for a first-order wall reaction is given by Eq. (B-4). Its counterpart for a second-order wall reaction can be obtained by generalizing the theory of Ref. 7 to allow for second-order reactions. This generalization was carried through to the point of identifying the similarity parameter,



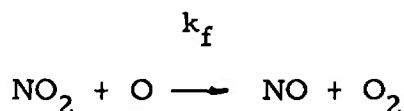
$$G_2 = 1.2373 S_c^{2/3} \frac{\rho_w^2 \alpha_2 k_{w2}}{\rho_e u_e} \sqrt{\frac{Re_{x_0}}{C}} \quad (B-7)$$

It is important to note in connection with Eq. (B-4) and (B-7) that  $k_{w1} \neq k_{w2}$ . The former has the dimensions of a velocity while the latter has the dimensions of velocity/density.

There is no reference in the literature to catalytic wall reactions in air when two reactants are present, but there are two mechanisms that appear plausible on the basis of gas-phase reactions. The first is based on the observation that the catalytic surface is conditioned using dissociated oxygen, and hence atomic oxygen is the adsorbed reactant. In the gas phase, the reaction,



is about two orders of magnitude faster than the three-body oxygen recombination. It can be hypothesized that in the corresponding wall reaction, the NO would react with the adsorbed O atoms to form NO<sub>2</sub> which would then desorb and dissociate in the boundary layer in the rapid rearrangement reaction,



With this mechanism, the mass fractions in Eq. (B-7) would be  $\alpha_1 = \alpha_2$  and  $\alpha_2 = \alpha_{\text{NO}}$ .

The second mechanism that seems plausible is that the nitric oxide rapidly reacts with the adsorbed O atoms to form NO<sub>2</sub>, and the NO<sub>2</sub> then remains adsorbed and participates in the above rearrangement reaction, followed by both products being desorbed and replaced by an O atom. In this mechanism, the gaseous concentration of NO would remain unchanged and the NO would only provide a reaction path. In this case, both  $\alpha_1$  and  $\alpha_2$  would be the atomic oxygen mass fractions.

## REFERENCES

1. Vidal, R. J. and Golian, T. C. , "Heat Transfer Measurements with a Catalytic Flat Plate in Dissociated Oxygen, " AIAA Paper 67-163, Jan. 1967; also AIAA J. , Vol. 5, No. 9, pp. 1579-1588, Sept. 1967.
2. Vidal, R. J. , "Species Diffusion in the Frozen Laminar Boundary Layer on a Catalytic Flat Plate, " CAL Rept. AG-1905-A-2, AEDC-TR-67-88, April 1967.
3. Bartz, J. A. , "Heat Transfer Measurements with a Catalytic Flat Plate in a Nonequilibrium Expansion of Oxygen, " CAL Rept. AG-1905-A-3, AEDC-TR-67-249, Nov. 1967.
4. Hartunian, R. A. and Thompson, W. P. , "Nonequilibrium Stagnation Point Heat Transfer Including Surface Catalysis, " AIAA Paper 63-464, 1963.
5. Crocco, L. , "A Characteristic Transformation of the Equations of the Boundary Layer in Gases, " Atti di Guidonia I, No. 6, 1939; translated in Aeronautical Research Council Rept. 4582.
6. Young, A. D. , Modern Developments in Fluid Dynamics -- High Speed Flow, edited by L. Howarth (Oxford Univ. Press, London, 1953), Vol. 1, pp. 378-431.
7. Chung, P. M. , Liu, S. W. , and Mirels, H. , "Effect of Discontinuity of Surface Catalycity on Boundary Layer Flow of Dissociated Gas, " Int. J. Heat Mass Transfer, Vol. 6, No. 3, pp. 193-210, March 1963.
8. Simpkins, P. G. , "Diffusion of Species over Surfaces With Discontinuous Catalycity, " Phys. Fluids, Vol. 9, No. 6, pp. 1241-1245, June 1966.
9. Greaves, J. C. and Linnett, J. W. , "The Recombination of Oxygen Atoms at Surfaces, " Trans. Faraday Soc. , Vol. 54, No. 429, Pt. 9, pp. 1323-1330, Sept. 1958.

10. Hartunian, R. A. , Thompson, W. P. , and Safron, S. , "Measurements of Catalytic Efficiency of Silver for Oxygen Atoms and the O-O<sub>2</sub> Diffusion Coefficient," J. Chem. Phys. , Vol. 43, No. 11, pp. 4003-4006, 1 Dec. 1965.
11. Myerson, A. L. , "Surface Recombination Efficiencies in Flows Containing Step-Function Increases in Atomic Oxygen," CAL Rept. AF-2033-A-1, AFOSR 68-0893, March 1968.
12. Marrone, P. V. , "Inviscid, Nonequilibrium Flow behind Bow and Normal Shock Waves, Part I. General Analysis and Numerical Examples," CAL Rept. QM-1626-A-12(I), May 1963.
13. Vidal, R. J. , "A Solution for Gas-Phase Recombination and Dissociation in the Laminar Boundary Layer of a Flat Plate," CAL Rept. AF-2753-A-1, Nov. 1969.
14. Lordi, J. A. and Mates, R. E. , "Nonequilibrium Effects on High-Enthalpy Expansions of Air," AIAA J. , Vol. 3, No. 10, pp. 1972-1974, Oct. 1965.
15. Stollery, J. L. and Smith, J. E. , "A Note on the Variation of Vibrational Temperature along a Nozzle," J. Fluid Mech. , Vol. 13, Part 2, pp. 225-236, June 1962.
16. Cheng, H. K. , Hall, J. G. , Golian, T. C. , and Hertzberg, A. , "Boundary-Layer Displacement and Leading Edge Bluntness Effects in High-Temperature Hypersonic Flow," J. Aero/Space Sci. , Vol. 28, No. 5, pp. 353-381, May 1961.
17. Rae, W. J. , "A Solution for the Nonequilibrium Flat-Plate Boundary Layer," AIAA J. , Vol. 1, No. 10, pp. 2279-2288, Oct. 1963.
18. Kaufman, F. , Chap. 14, "Neutral Reactions." In DASA Reaction Rate Handbook, DASA 1948. Prepared by General Electric Co. , Missile and Space Div. , Space Sciences Lab. , Oct. 1967.
19. Chapman, D. R. and Rubesin, M. W. , "Temperature and Velocity Profiles in the Compressible Laminar Boundary Layer with Arbitrary Distribution of Surface Temperature," J. A. S. , Vol. 16, No. 9, pp. 547-565, Sept. 1949.

20. Eckert, E. R. G. and Drake, R. M. , Heat and Mass Transfer, McGraw Hill, New York, 1959.
21. Vidal, R. J. , Skinner, G. T. , and Bartz, J. A. , "Speed-Ratio Measurements in Nonequilibrium Nozzle and Free-Jet Expansions, " Rarefied Gas Dynamics, Supplement 4, Vol. II, C. L. Brundin, Editor. Academic Press, New York, pp. 1287-1316, 1967.
22. Hall, J. G. , Eschenroeder, A. Q. , and Marrone, P. V. , "Blunt-Nose Inviscid Airflows with Coupled Nonequilibrium Processes, " J. Aerospace Sci. , Vol. 29, No. 9, pp. 1038-1051, Sept. 1962.
23. Byron, S. B. , "Interferometric Measurement of the Rate of Dissociation of Oxygen Heated by Strong Shock Waves, " Cornell Univ. Rept. 1958; J. Chem. Phys. , Vol. 30, pp. 1380-1392, 1959.
24. Wray, K. L. , Teare, J. D. , Kivel, B. , and Hammerling, P. , "Relaxation Processes and Reaction Rates behind Shock Fronts in Air and Component Gases, " AVCO Res. Rept. 83, Dec. 1959.
25. Glick, H. S. , Klein, J. J. , and Squire, W. J. , Single-Pulse Shock Tube Studies of the Kinetics of the Reaction  $\text{N}_2 + \text{O}_2 \rightleftharpoons 2\text{NO}$  between 2000-3000°K, " J. Chem. Phys. , Vol. 27, p. 850, 1957.
26. Wray, K. L. , "Chemical Kinetics of High Temperature Air, " Hypersonic Flow Research--Progress in Astronautics and Rocketry, Vol. 7, pp. 181-204; Academic Press, New York, 1962.
27. Laidler, K. J. , "Kinetic Laws in Surface Catalysis, " Catalysis, Fundamental Principles, Vol. I. Reinhold Publishing Corp. , New York, 1954.

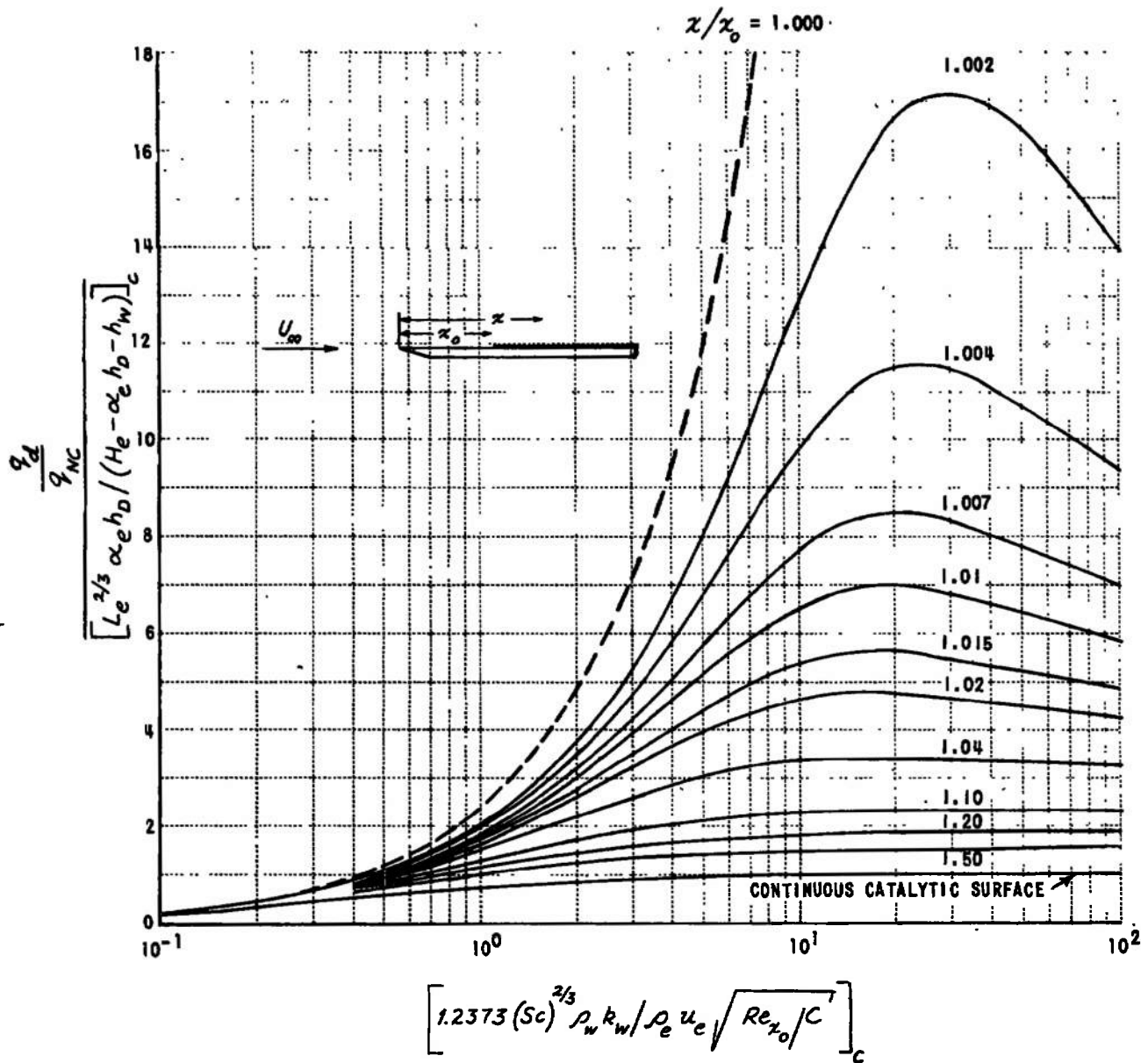


Figure 1 THEORY FOR HEAT TRANSFER TO A SURFACE WITH A DISCONTINUOUS CATALYTIC EFFICIENCY - REF. 7

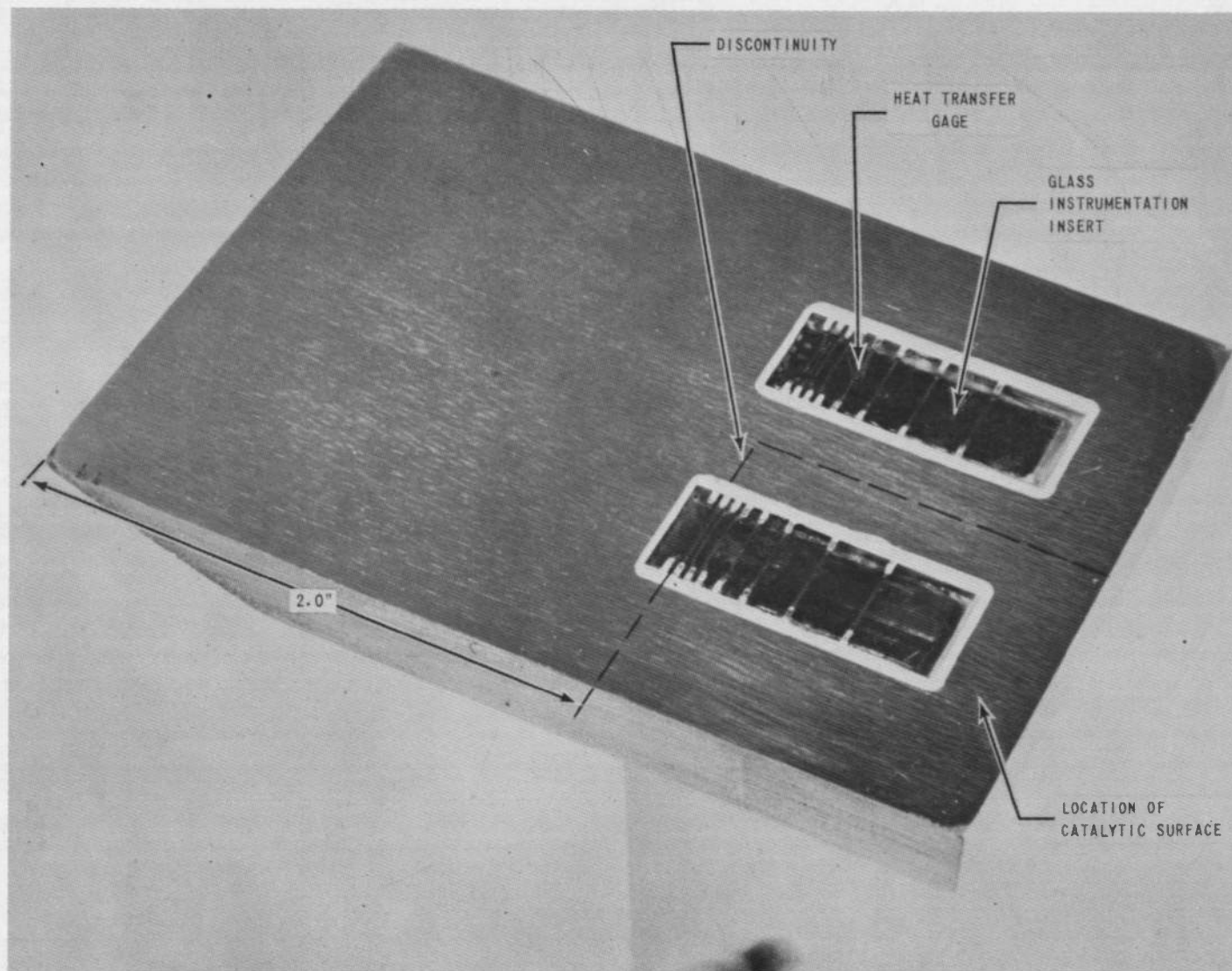


Figure 2a SMALL SCALE CATALYTIC PROBE

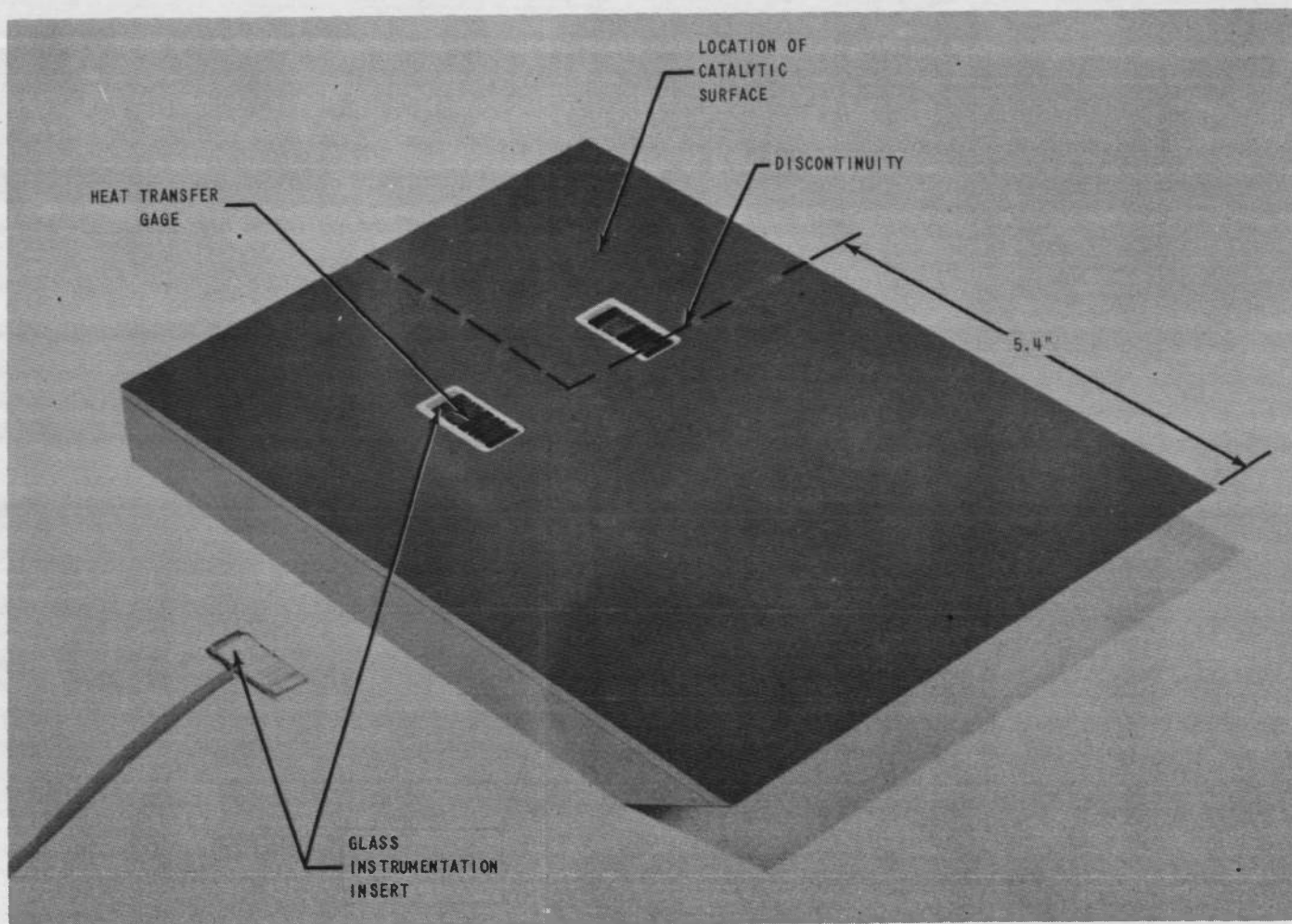


Figure 2b LARGE SCALE CATALYTIC PROBE

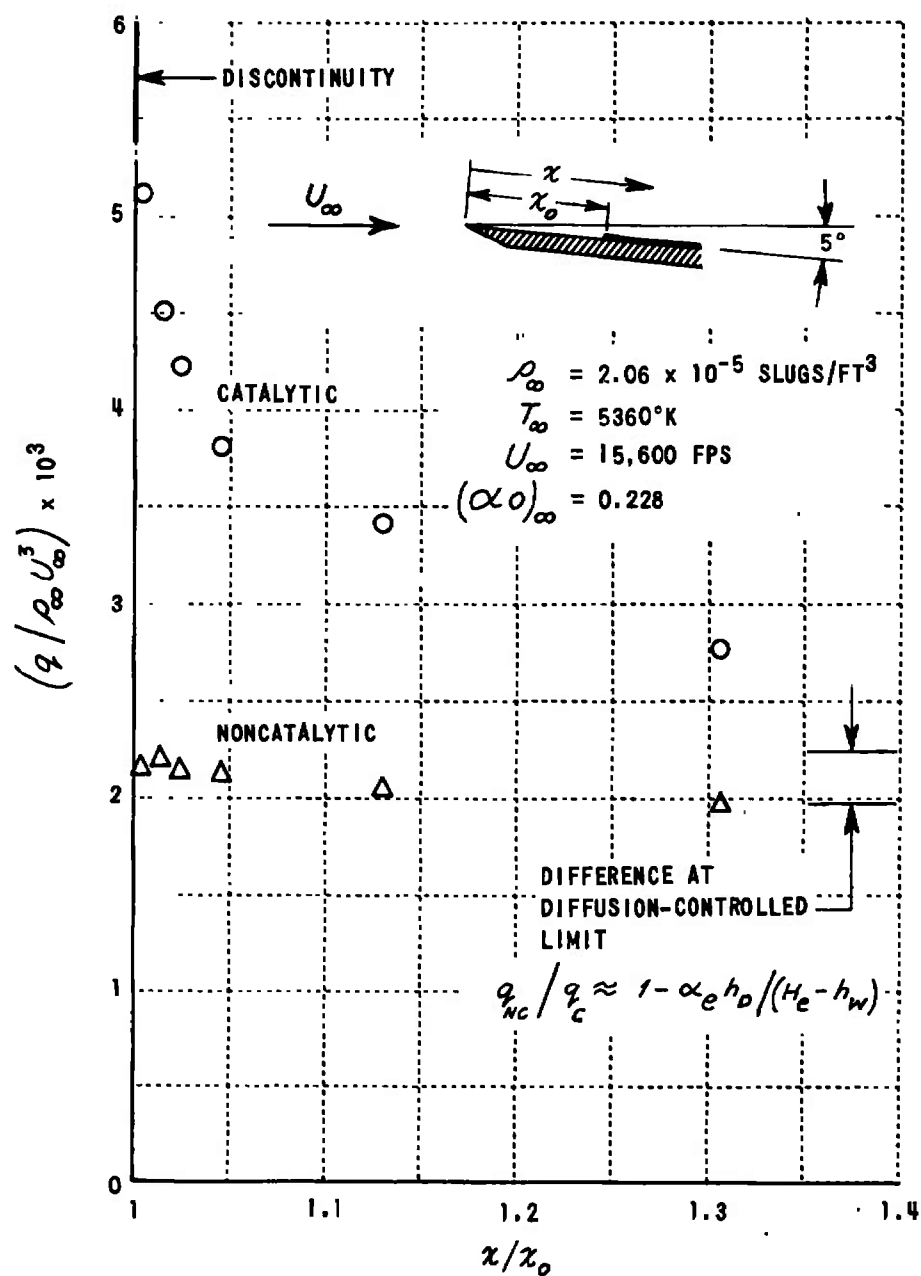


Figure 3 TYPICAL DATA OBTAINED WITH A CATALYTIC PROBE  
IN AN EQUILIBRIUM AIRFLOW



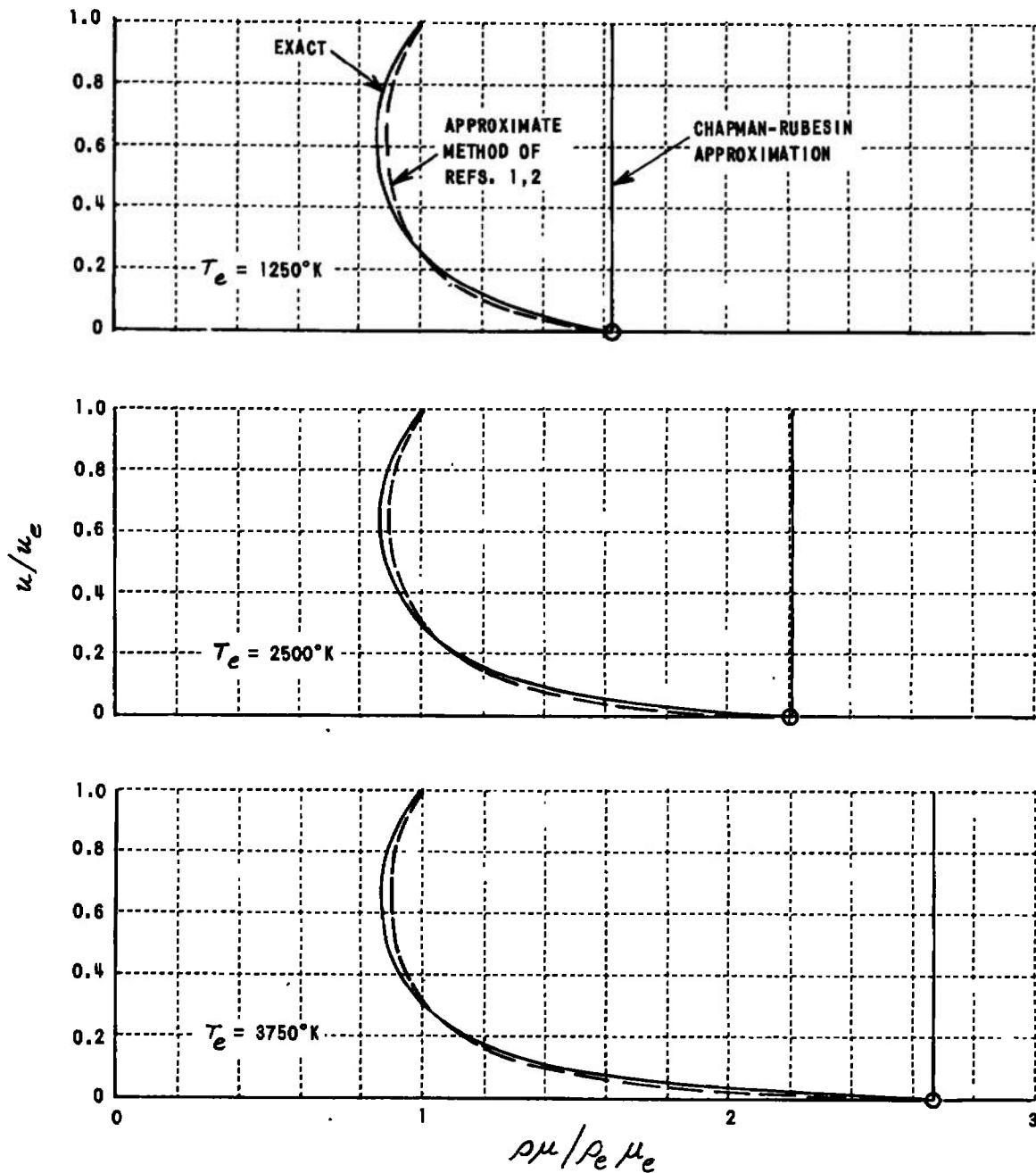


Figure 4 VARIATION OF THE DENSITY-VISCOSITY PRODUCT IN AIR ACROSS A BOUNDARY LAYER (BLASIUS PROFILE)

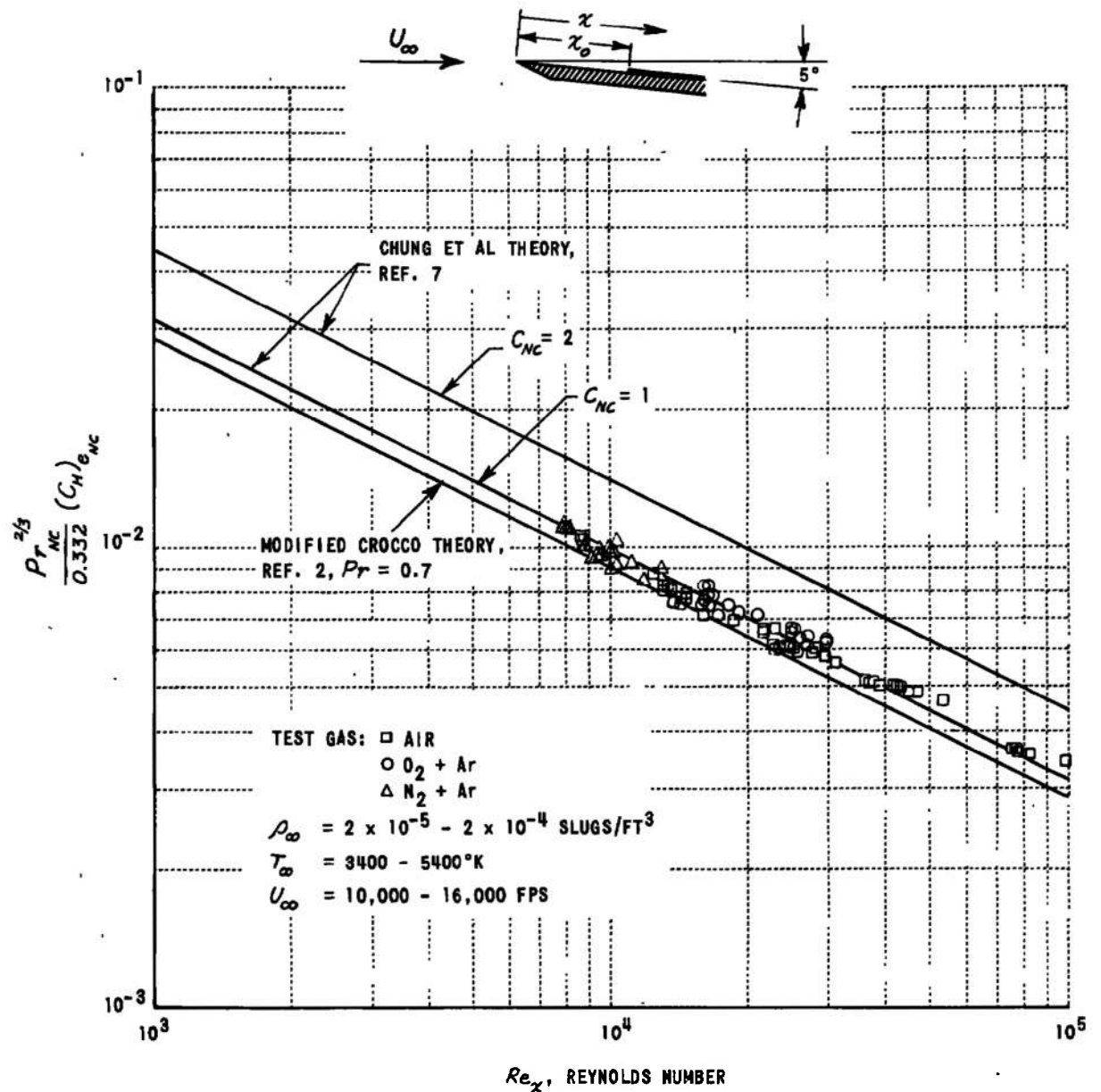


Figure 5 CONVECTIVE HEAT TRANSFER TO A FLAT PLATE IN EQUILIBRIUM FLOW

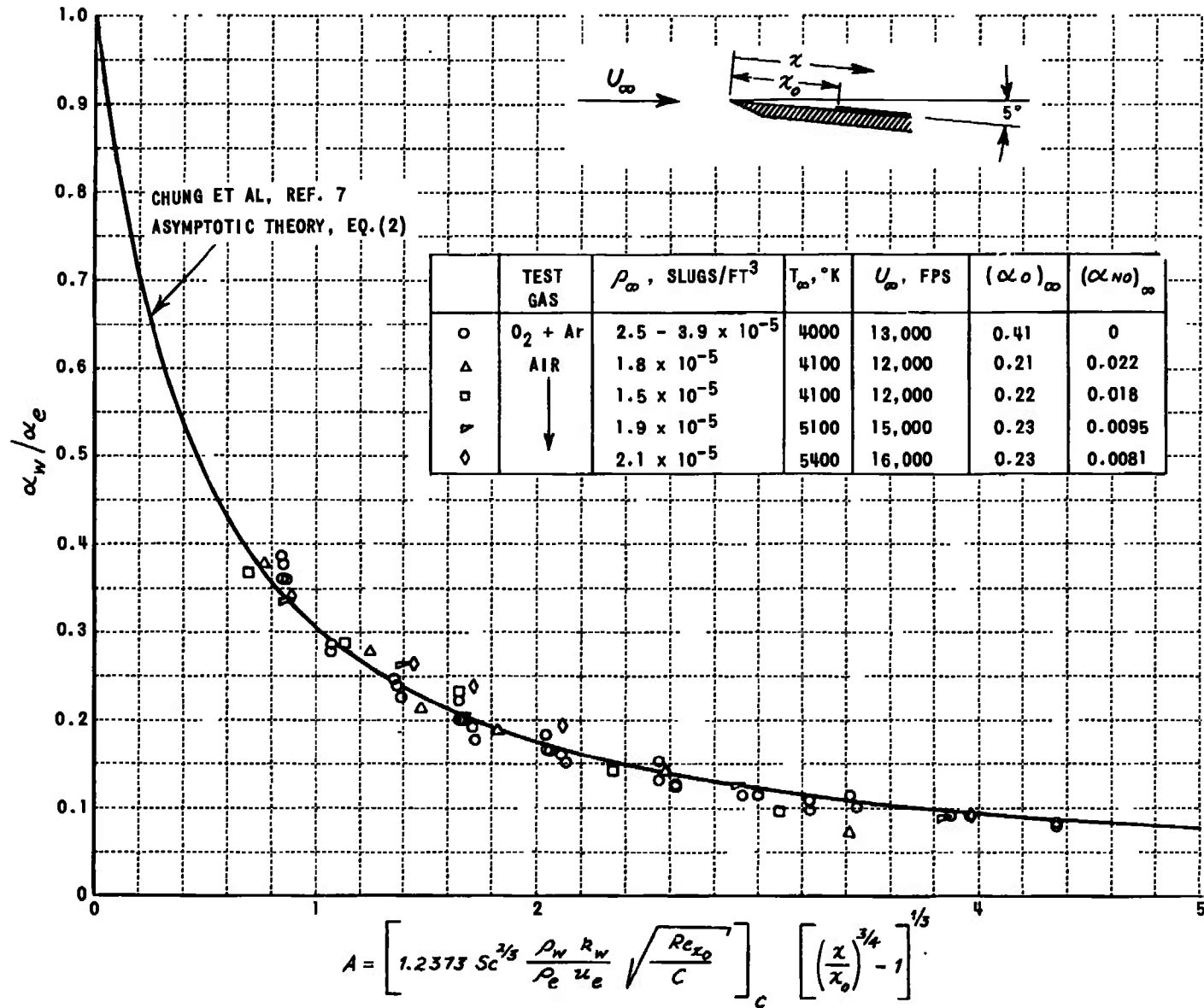


Figure 6 COMPARISON OF THEORETICAL AND MEASURED ATOM FRACTIONS ON A CATALYTIC SURFACE IN EQUILIBRIUM FLOWS

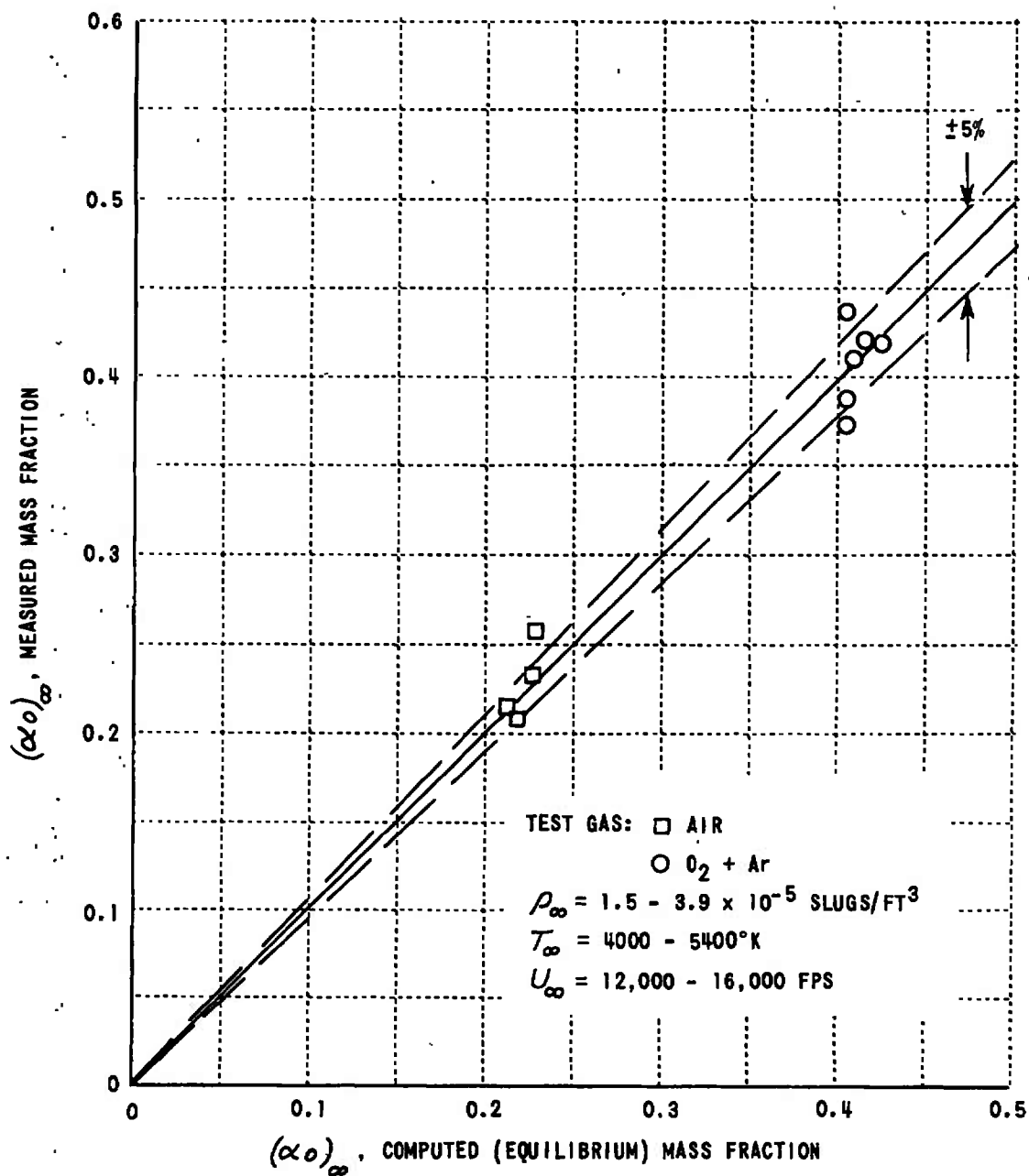


Figure 7 AMBIENT OXYGEN ATOM FRACTIONS INFERRED WITH A CATALYTIC PROBE IN EQUILIBRIUM FLOWS

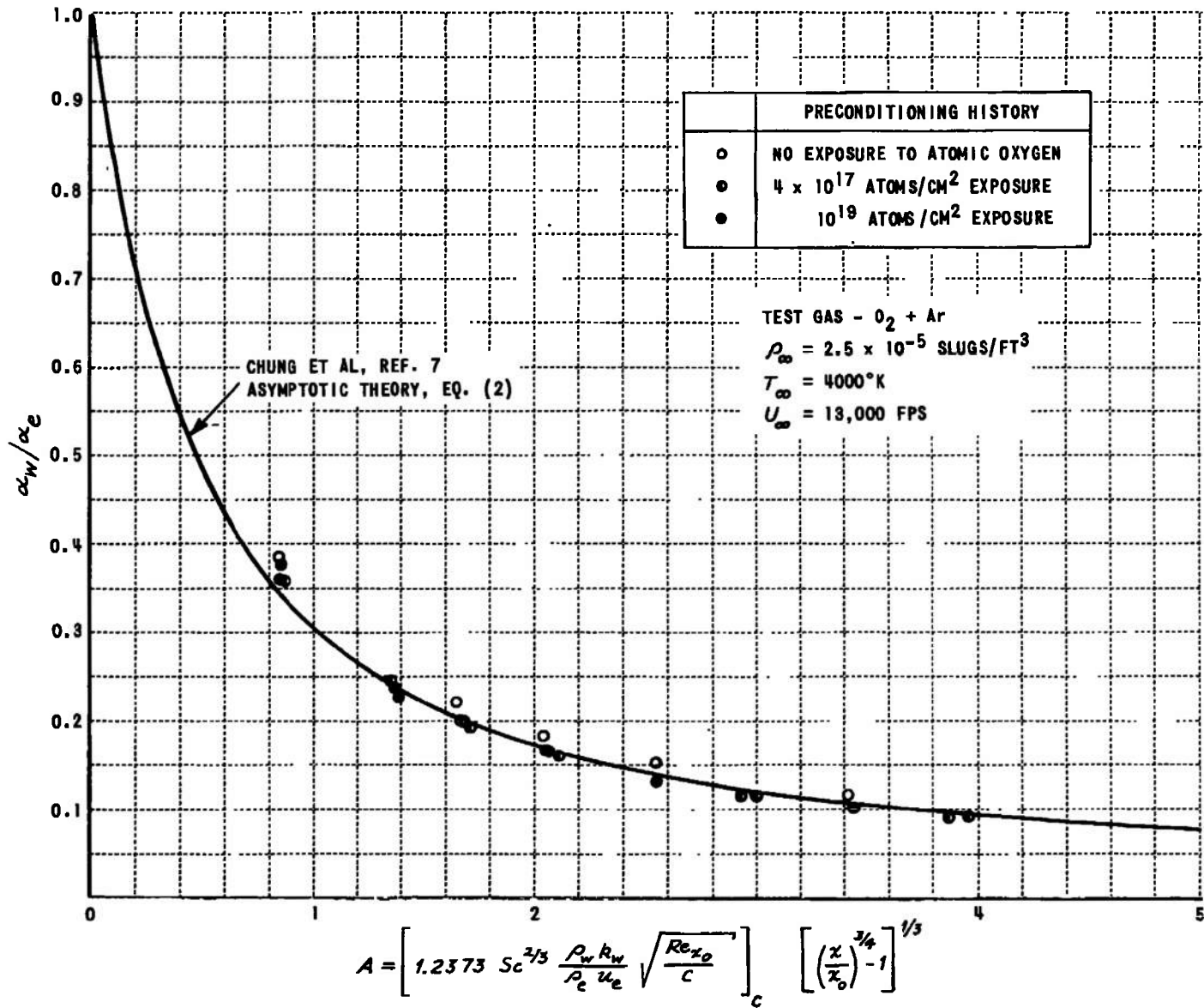


Figure 8 EFFECT OF PRECONDITIONING ON THE CATALYTIC SURFACE

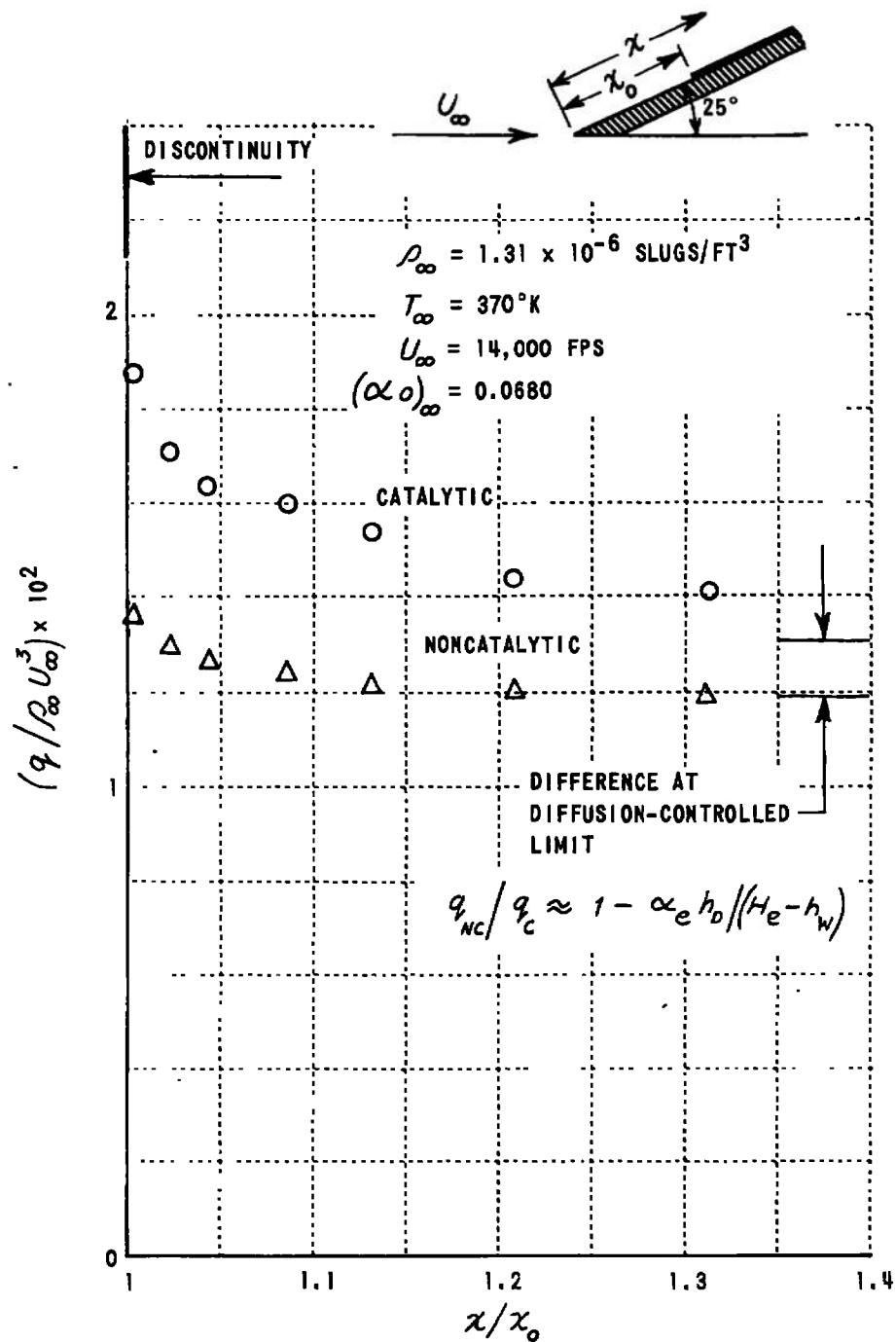


Figure 9 TYPICAL DATA OBTAINED WITH A CATALYTIC PROBE IN A NONEQUILIBRIUM AIRFLOW

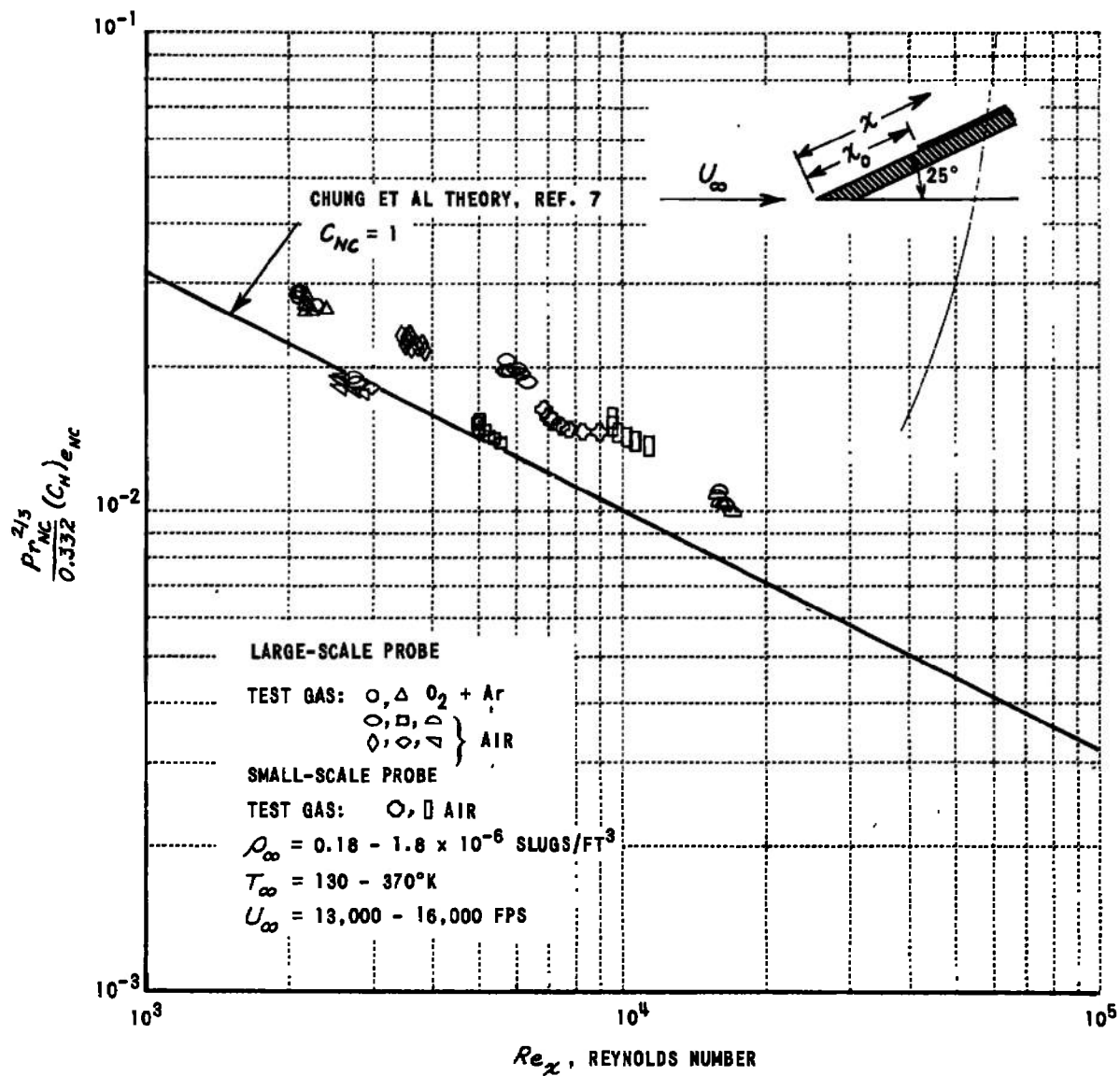


Figure 10 CONVECTIVE HEAT TRANSFER TO A WEDGE IN NONEQUILIBRIUM FLOW

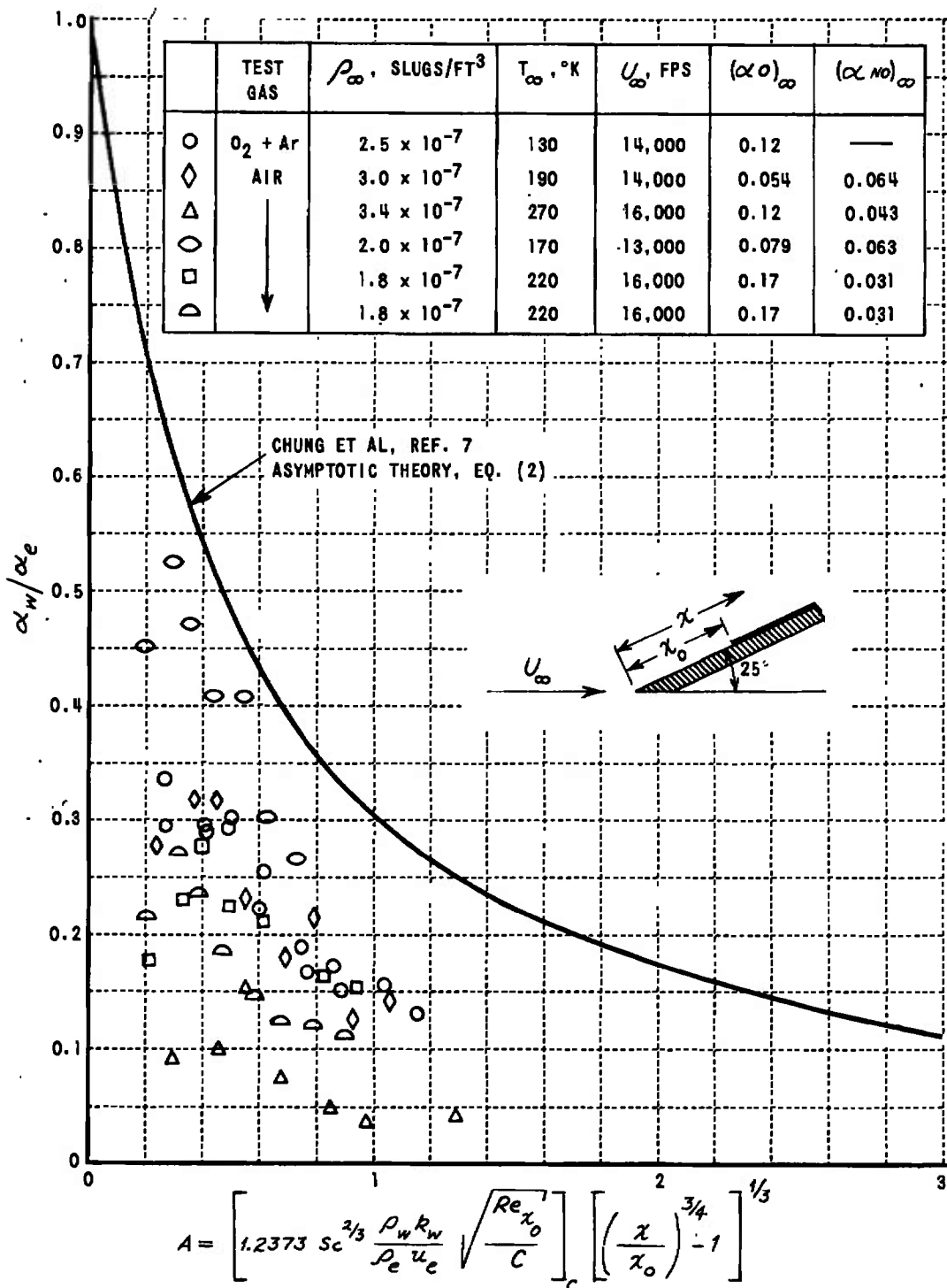


Figure 11 COMPARISON OF THEORETICAL AND MEASURED ATOM FRACTIONS ON A CATALYTIC SURFACE IN NONEQUILIBRIUM NOZZLE FLOWS - LARGE-SCALE PROBE



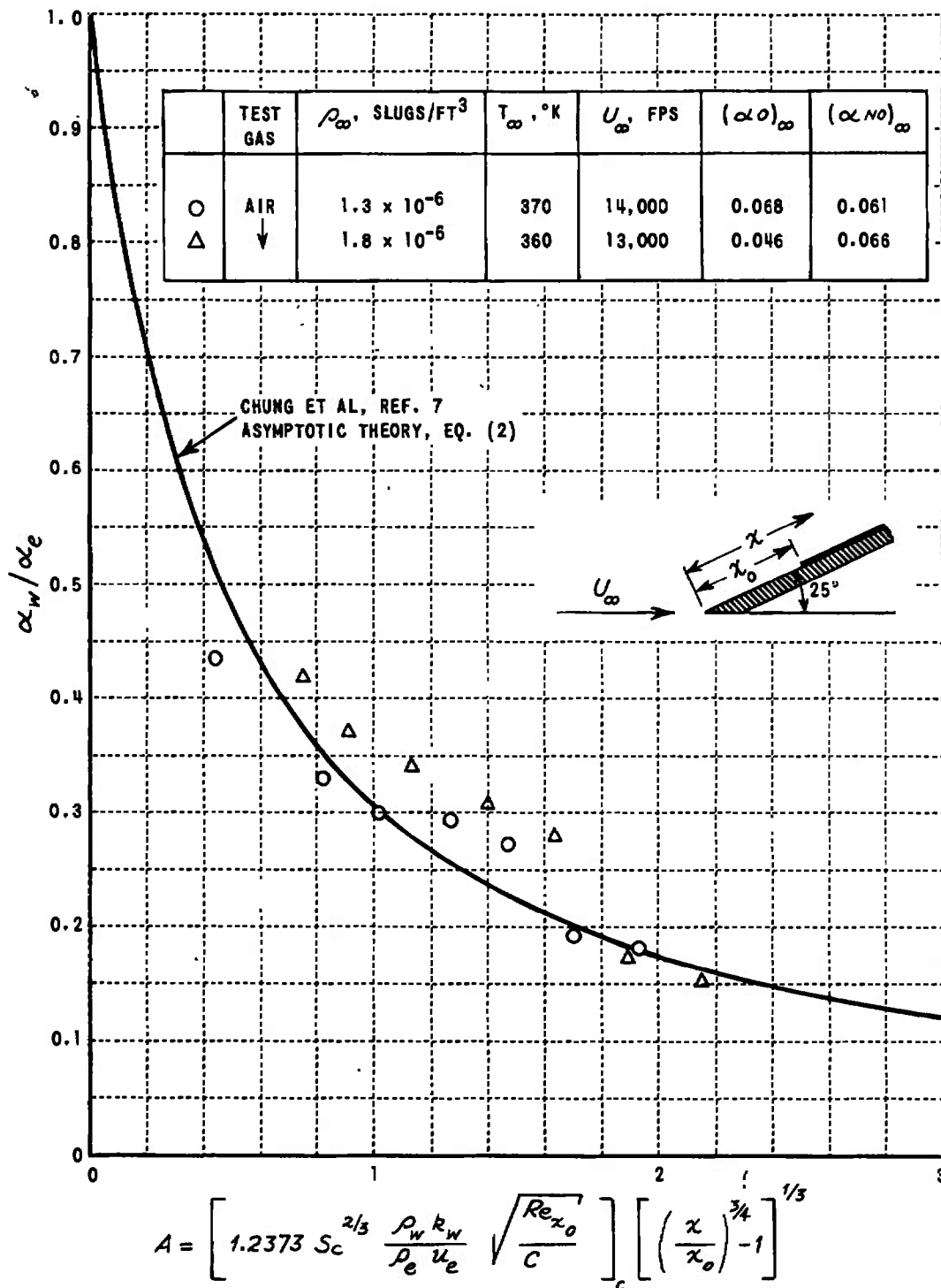


Figure 12 COMPARISON OF THEORETICAL AND MEASURED ATOM FRACTIONS ON A CATALYTIC SURFACE IN NONEQUILIBRIUM NOZZLE FLOWS - SMALL-SCALE PROBE

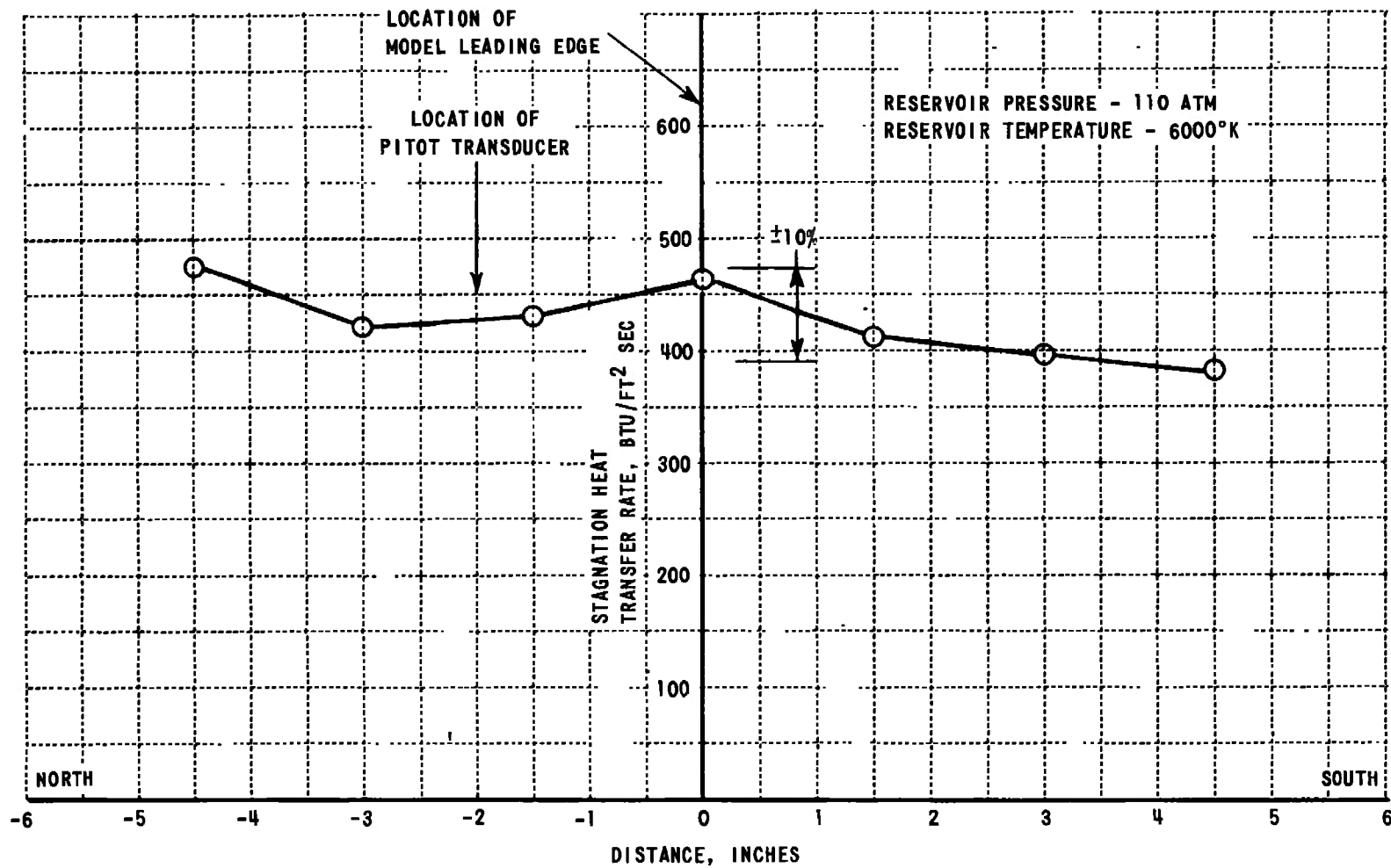


Figure 13a SURVEY OF NOZZLE FLOW UNIFORMITY

50

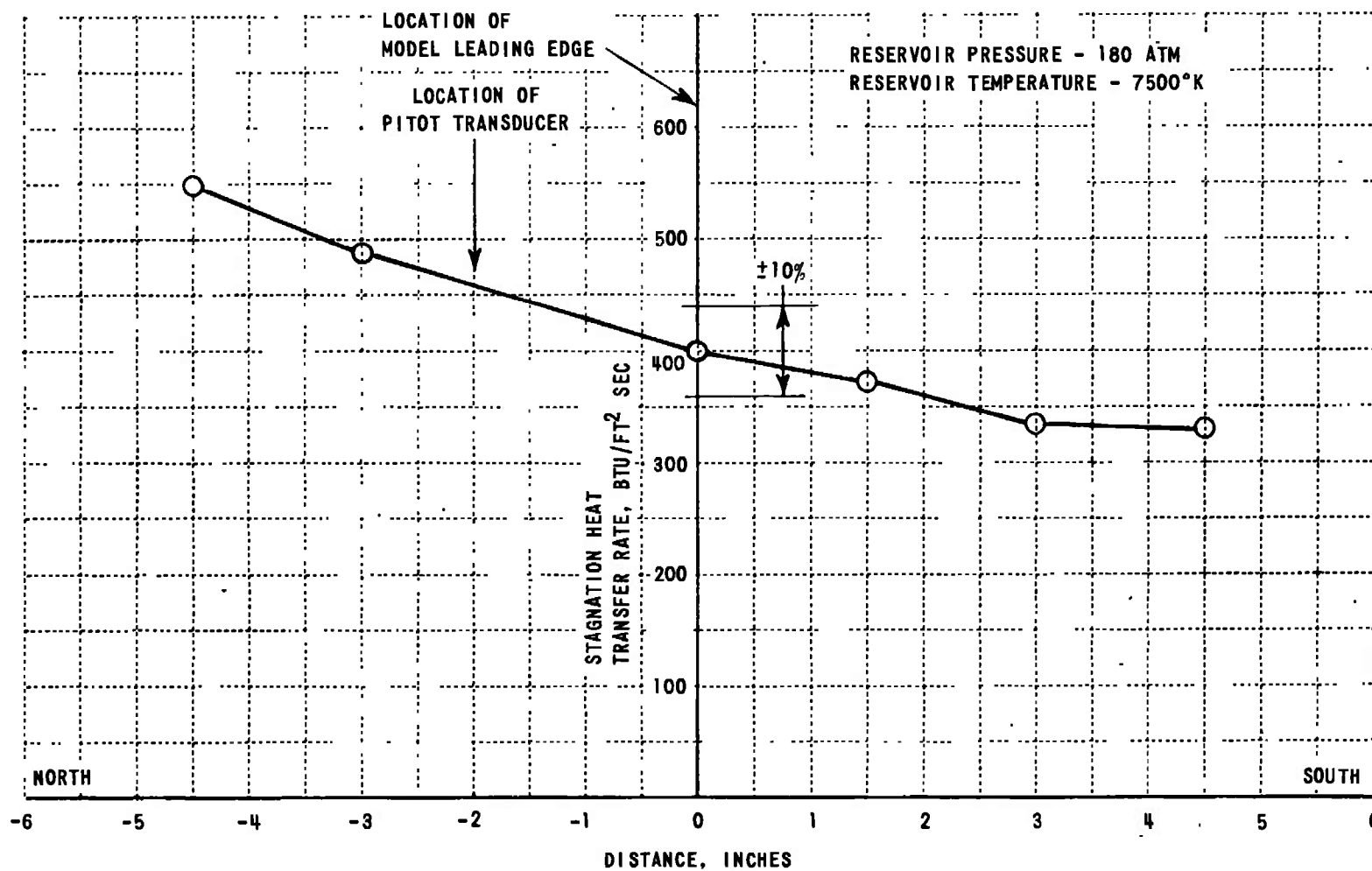


Figure 13b SURVEY OF NOZZLE FLOW UNIFORMITY

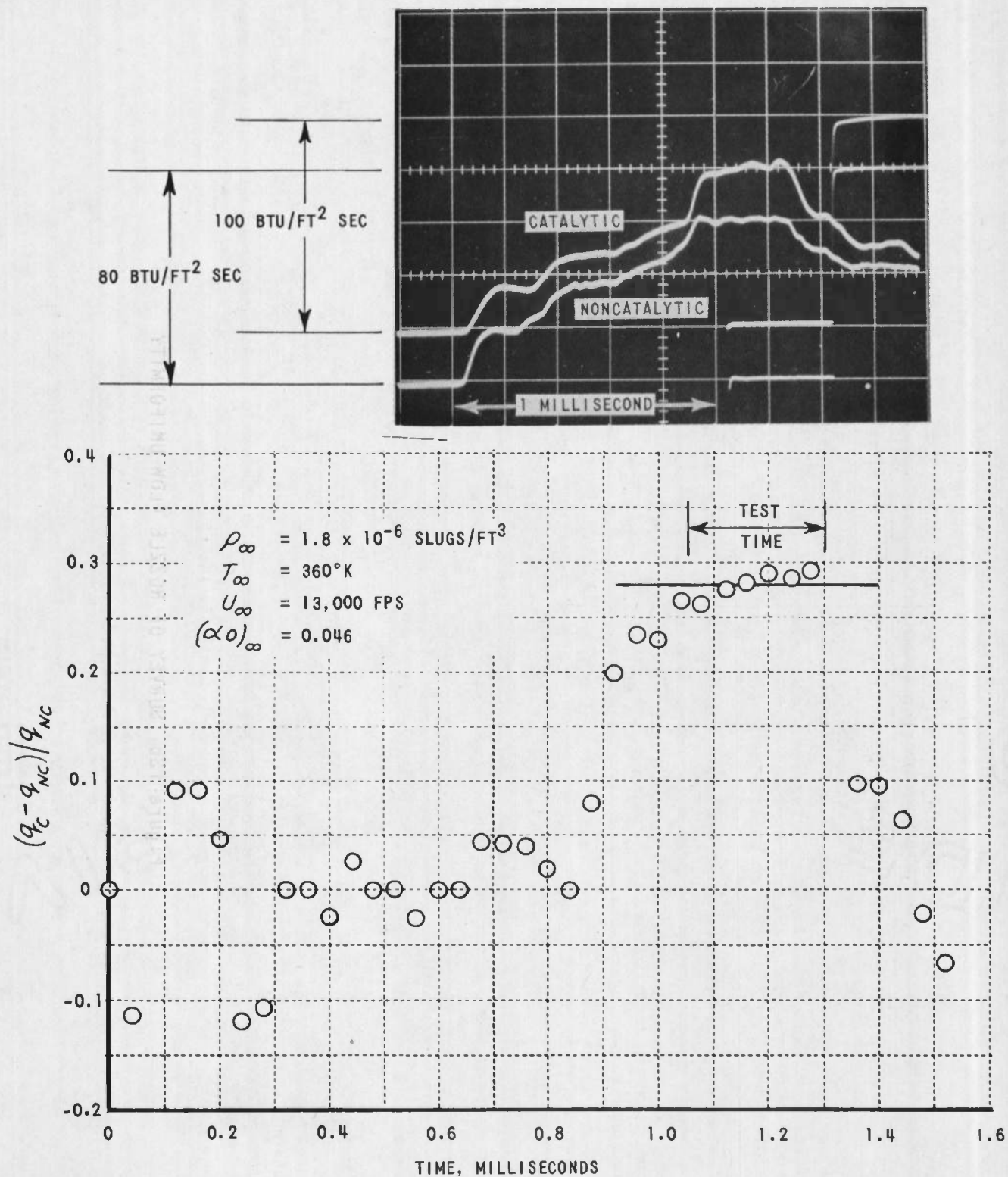


Figure 14 THE TEMPORAL VARIATION OF INFERRED ATOM FRACTION

UNCLASSIFIED

Security Classification

## DOCUMENT CONTROL DATA - R &amp; D

(Security classification of title, body of abstract and indexing annotation must be entered when the overall report is classified)

## 1. ORIGINATING ACTIVITY (Corporate author)

Cornell Aeronautical Laboratory, Inc.  
Aerodynamic Research Department  
Buffalo, New York 14221

## 2a. REPORT SECURITY CLASSIFICATION

UNCLASSIFIED

## 2b. GROUP

N/A

## 3. REPORT TITLE

RESEARCH ON SURFACE CATALYSIS IN NONEQUILIBRIUM FLOWS

## 4. DESCRIPTIVE NOTES (Type of report and inclusive dates)

Final Report - September 1967 to September 1969

## 5. AUTHOR(S) (First name, middle initial, last name)

John A. Bartz and Robert J. Vidal

## 6. REPORT DATE

April 1970

## 7a. TOTAL NO. OF PAGES

59

## 7b. NO. OF REFS

27

## 8a. CONTRACT OR GRANT NO.

F40600-68-C-0001 and F40600-69-C-  
b. PROJECT NO. 8951 0005

c. Task 895106

d.

## 9a. ORIGINATOR'S REPORT NUMBER(S)

AEDC-TR-70-111

## 9b. OTHER REPORT NO(S) (Any other numbers that may be assigned this report)

AF-2753-A-2

## 10. DISTRIBUTION STATEMENT

This document has been approved for public release and sale;  
its distribution is unlimited.

## 11. SUPPLEMENTARY NOTES

Available in DDC

## 12. SPONSORING MILITARY ACTIVITY

Arnold Engineering Development  
Center (AEL), Air Force Systems Com-  
mand, Arnold AF Sta., Tenn. 37389

## 13. ABSTRACT

This report describes the results of a program of research to develop a catalytic probe with a discontinuous catalytic surface. The ultimate objective is to use the probe to measure the ambient oxygen atom concentrations in high-temperature wind tunnel facilities, and a discontinuous catalytic surface was used to increase the probe sensitivity to small atom concentrations. This report first reviews the theoretical basis for this probe configuration, and then presents experimental data obtained with the probe in air and simulated air. The accuracy of existing theory for a probe with a discontinuous catalytic surface is demonstrated in equilibrium flow experiments in a shock tube using simulated air with a single reactant. Subsequent equilibrium flow experiments in real air indicate that oxygen atom recombination is the only important reaction occurring on the surface and thereby demonstrate the utility of the probe as a diagnostic in high-temperature air flows. Exploratory experiments are described using the catalytic probe in a nonequilibrium flow of air and simulated air produced in a shock tunnel. These results show large discrepancies between theory and experiment, and the possible sources of these discrepancies are discussed. It is concluded that the discrepancies could result from a weak wave system in the nozzle and from uncertainties in the chemical rate data used in the theoretical prediction of the nozzle flow.

UNCLASSIFIED

Security Classification

14.

KEY WORDS

catalytic probe  
heat transfer  
flat plates

LINK A

LINK B

LINK C

ROLE

WT

ROLE

WT

ROLE

WT

UNCLASSIFIED

Security Classification